Molecular Cell
Article

Nuclear FAK Promotes Cell Proliferation and Survival through FERM-Enhanced p53 Degradation

Ssang-Taek Lim,[1] Xiao Lei Chen,[1] Yangmi Lim,[1] Dan A. Hanson,[1] Thanh-Trang Vo,[1,3] Kyle Howerton,[2,4] Nicholas Larocque,[2] Susan J. Fisher,[2] David D. Schlaepfer,[1,*] and Dusko Ilic[2,5]
[1]Department of Reproductive Medicine, Moores Cancer Center, University of California, San Diego, 3855 Health Sciences Drive, MC0803, La Jolla, CA 92093, USA
[2]Department of Cell and Tissue Biology, University of California, San Francisco, 513 Parnassus Avenue, Box 0512, HSW-604, San Francisco, CA 94143, USA
[3]Present address: Graduate School of Arts and Sciences, Harvard University, 1350 Massachusetts Avenue, Holyoke Center 350, Boston, MA 02138, USA.
[4]Present address: PrimeGen Biotech LLC, 213 Technology Drive, Irvine, CA 92618, USA.
[5]Present address: StemLifeLine Inc., 1300 Industrial Road, Number 13, San Carlos, CA 94070, USA.
*Correspondence: dschlaepfer@ucsd.edu
DOI 10.1016/j.molcel.2007.11.031

SUMMARY

FAK is known as an integrin- and growth factor-associated tyrosine kinase promoting cell motility. Here we show that, during mouse development, FAK inactivation results in p53- and p21-dependent mesodermal cell growth arrest. Reconstitution of primary FAK$^{-/-}$p21$^{-/-}$ fibroblasts revealed that FAK, in a kinase-independent manner, facilitates p53 turnover via enhanced Mdm2-dependent p53 ubiquitination. p53 inactivation by FAK required FAK FERM F1 lobe binding to p53, FERM F2 lobe-mediated nuclear localization, and FERM F3 lobe for connections to Mdm2 and proteasomal degradation. Staurosporine or loss of cell adhesion enhanced FERM-dependent FAK nuclear accumulation. In primary human cells, FAK knockdown raised p53-p21 levels and slowed cell proliferation but did not cause apoptosis. Notably, FAK knockdown plus cisplatin triggered p53-dependent cell apoptosis, which was rescued by either full-length FAK or FAK FERM re-expression. These studies define a scaffolding role for nuclear FAK in facilitating cell survival through enhanced p53 degradation under conditions of cellular stress.

INTRODUCTION

Integrins are transmembrane receptors that mediate cell attachment to ECM and also cooperate with growth factor receptors to generate intracellular signals regulating growth and survival. Disruption of these signals can trigger cell-cycle arrest or apoptosis (Gilmore, 2005). One of the executioners of these events is the p53 tumor suppressor protein (Reddig and Juliano, 2005). Under steady-state growth conditions, p53 expression is maintained at low levels via polyubiquitination and proteasomal degradation (Vousden, 2002). Murine double minute-2 (Mdm2) is one of several ubiquitin E3 ligases that regulate p53 levels in cells (Iwakuma and Lozano, 2003). Activation of p53 in response to stress signals is associated with increased p53 stability (Harris and Levine, 2005) leading to the enhanced transcription of targets such as p21Cip/WAF1 (p21) cyclin-dependent kinase inhibitor (Oren, 2003). ECM-integrin signals can counteract p53 activation (Stromblad et al., 1996) and enhance proteasomal degradation of p21 (Bao et al., 2002), but regulatory connections between integrins and p53 are not clear.

Focal adhesion kinase (FAK) and the related Pyk2 kinase are cytoplasmic tyrosine kinases activated by integrins and growth factor receptors (Parsons, 2003). FAK inactivation during development yields an embryonic lethal phenotype, and the growth of FAK$^{-/-}$ fibroblasts and endothelial cells is facilitated by p53 inactivation (Ilic et al., 1995, 1998, 2003). Although integrin-stimulated FAK autophosphorylation at Y397, Src-family PTK binding to FAK pY397, and the formation of a FAK-Src signaling complex promote cell motility and cell survival, (Cox et al., 2006; Mitra and Schlaepfer, 2006), the connections between FAK and p53 regulation remain loosely defined.

Recent studies have elucidated the structure of the FAK N-terminal band 4.1, ezrin, radixin, moesin homology (FERM) domain, which is comprised of three distinct lobes (F1, F2, and F3) (Lietha et al., 2007) and acts to regulate FAK kinase activity through an intramolecular inhibitory mechanism (Cohen and Guan, 2005; Lietha et al., 2007). Interestingly, FAK can be modified by small ubiquitin-related modifier (SUMO) addition at K152 within the FERM domain (Kadare et al., 2003), SUMOylated FAK is nuclear enriched, and exogenous FAK FERM expression is nuclear localized (Golubovskaya et al., 2005; Stewart et al., 2002). Despite reports of FAK in the nucleus, the mechanism(s) that promotes or regulates FAK nuclear accumulation and the biological role of nuclear FAK remains unknown.

Here we show that loss of FAK activates p53 during mouse embryogenesis and that FAK$^{-/-}$ embryo cell proliferation ex vivo is made possible by either p53 or p21 inactivation. Although FAK has been proposed to inhibit p53 transcriptional activity (Golubovskaya et al., 2005), we find that the MG132 proteosomal inhibitor blocks FAK regulation of p53. We show that FAK inactivates p53 in a kinase-independent manner via the FAK FERM

domain acting as a scaffold to enhance Mdm2-dependent p53 ubiquitination. Although FERM domain SUMOylation is not required, p53 regulation is dependent on FAK nuclear translocation. Importantly, DNA damage-associated cell apoptosis could be rescued by wild-type (WT) but not nuclear-excluded FAK FERM re-expression after FAK knockdown in human fibroblasts. These results support a biological role for nuclear FAK in promoting cell proliferation and survival by facilitating p53 turnover.

RESULTS

Mesoderm Proliferation Defects in E8.5 FAK$^{-/-}$ Mouse Embryos

The *fak* knockout results in an early embryonic lethal (E8.5) phenotype (Ilic et al., 1995) and size comparisons between normal FAK$^{+/+}$, FAK$^{+/-}$, and FAK$^{-/-}$ littermates at E8.0–8.5 show that both FAK$^{+/-}$ and FAK$^{-/-}$ embryos are smaller than FAK$^{+/+}$ embryos (Figure 1A). By E11.5, FAK$^{+/-}$ embryos become indistinguishable from FAK$^{+/+}$ embryos, whereas FAK$^{-/-}$ embryos do not survive beyond E8.5–9.0 (Ilic et al., 1995). To evaluate relative levels of cell proliferation during development, head-fold regions of FAK$^{+/+}$ and FAK$^{-/-}$ littermate embryos were immunostained with antibodies to phosphorylated serine 10 histone H3 (pHis3) (Figure 1B). Equal numbers of pHis3-stained head-fold ectoderm cells were detected in FAK$^{+/+}$ and FAK$^{-/-}$ embryos (Figure 1C). In contrast, few pHis3-stained mesoderm cells were detected in FAK$^{-/-}$ compared to FAK$^{+/+}$ embryos (Figures 1B and 1C), supporting the notion that a proliferation defect induced by *fak* loss may occur in vivo.

p53 Accumulation Prevents FAK$^{-/-}$ Embryo Proliferation Ex Vivo

To elucidate the potential role of p53 in FAK$^{-/-}$ embryo growth defects, we evaluated p53 protein levels in E8.5 embryo lysates (Figure 1D). During development, p53 protein is rapidly turned over and not normally detected before E10.5–11.0 (Gottlieb et al., 1997). High levels of p53 and p53-responsive targets such as Mdm2 were detected in FAK$^{-/-}$ but not FAK$^{+/+}$ embryos, suggestive of p53 activation in the absence of FAK (Figure 1D). To evaluate the contribution of p53 in FAK$^{-/-}$ embryo growth, a p53$^{-/-}$ mutation was introduced onto the FAK$^{-/-}$ background by mating FAK$^{+/-}$ and p53$^{-/-}$ mice. p53 inactivation did not rescue the E8.5 embryonic lethality of FAK$^{-/-}$ embryos (data not shown). However, loss of p53 enabled primary FAK$^{-/-}$p53$^{-/-}$ embryo cell growth ex vivo, whereas FAK$^{-/-}$p53$^{+/+}$ cells failed to proliferate (Figures 1E and 1F). To quantify differences in cell growth, embryos were dissociated at day 6 ex vivo and cells cultured in the presence of bromodeoxyuridine (BrdU). Anti-BrdU staining revealed that FAK$^{+/+}$p53$^{+/+}$ and FAK$^{+/+}$p53$^{-/-}$ cells showed a similarly high rate of proliferation (50%–60%), whereas <2% of cells in FAK$^{-/-}$p53$^{+/+}$ embryos were BrdU positive (Figure 1F). Importantly, p53 inactivation released this proliferation block, resulting in ~70% BrdU-positive cells from FAK$^{-/-}$p53$^{-/-}$ embryos. This defect in FAK$^{-/-}$p53$^{+/+}$ embryo cell growth was not linked to the E8.0–8.5 time of extraction, as cell proliferation defects and DNA aberrations were observed in cultured E7.0–7.5 FAK$^{-/-}$p53$^{+/+}$ but not FAK$^{+/+}$p53$^{+/+}$ embryos (Figure 1G). Together, these results support the conclusion that p53 is active in FAK$^{-/-}$ embryos and that p53-associated signals block FAK$^{-/-}$ cell proliferation.

p53-Associated Proliferation Block in FAK$^{-/-}$ Cells Is p21 Dependent

To determine whether the absence of FAK results in changes in embryo protein expression, immunoblotting was performed on FAK$^{+/+}$, FAK$^{+/-}$, and FAK$^{-/-}$ E8.0–8.5 embryo lysates (Figure 2A). The upregulation of the FAK-related Pyk2 kinase was detected upon inactivation of one or both *fak* alleles. Comparisons of FAK$^{+/+}$ and FAK$^{-/-}$ embryo lysates showed decreases in cyclin B and cyclin E and increases in cyclin-dependent kinase inhibitors p57(Kip2), p27(Kip1), and p21(Cip1) in the absence of FAK (Figure 2A). These changes may reflect reduced cell proliferation within FAK$^{-/-}$ embryos; however, other cell-cycle-regulatory proteins such as p16(Ink4a) remained unchanged.

In cell culture, p21 expression is enhanced by disruption of ECM-integrin linkages (Bao et al., 2002) and inhibited by FAK signaling (Bryant et al., 2006). During embryogenesis, elevated p21 levels in the absence of FAK were dependent upon p53, as p21 expression was not detected in FAK$^{+/+}$, FAK$^{+/-}$, or FAK$^{-/-}$ embryos on a p53$^{-/-}$ background (Figure 2B). To test whether elevated p21 levels contribute to the p53-dependent block in FAK$^{-/-}$ embryo cell proliferation, a p21$^{-/-}$ mutation was introduced into a FAK$^{-/-}$p53$^{+/+}$ background by mating FAK$^{+/-}$ and p21$^{-/-}$ mice. FAK$^{-/-}$p21$^{-/-}$ mice exhibited embryonic lethality at ~E9.5 with increased mesoderm DNA fragmentation compared to FAK$^{+/+}$p21$^{-/-}$ littermates (Figure 2C). However, cells from E8.0–8.5 FAK$^{-/-}$p21$^{-/-}$ embryos proliferated ex vivo at ~75% the level of FAK$^{+/+}$p21$^{-/-}$ cells (Figures 2D and 2E). This release of the p53-dependent cell proliferation block was verified by BrdU incorporation into FAK$^{-/-}$p21$^{-/-}$p53$^{+/+}$ cells (~41%), but not FAK$^{-/-}$p21$^{+/+}$p53$^{+/+}$ cells (<2%) (Figure 2E). These studies support the notion that *fak* inactivation triggers a p53-p21-dependent cell proliferation block, yet release of this checkpoint is not sufficient to overcome an embryonic lethal FAK null phenotype.

FAK Promotes p53 Turnover via FAK FERM Domain-Enhanced p53 Ubiquitination

The inability of FAK$^{-/-}$p53$^{+/+}$ fibroblasts to grow in culture severely limits experimental analyses. To study the signaling linkage between FAK and p53, we generated FAK$^{-/-}$p21$^{-/-}$ and FAK$^{+/+}$p21$^{-/-}$ fibroblasts from E8.5 embryo littermates. In early passage FAK$^{-/-}$p21$^{-/-}$ cells, steady-state p53 levels were elevated, and transient FAK re-expression resulted in decreased p53 levels (see Figure S1A available online). This effect of FAK on p53 levels was associated with enhanced p53 turnover as determined by metabolic labeling of cells (Figures S1B–S1F).

To address which domains of FAK were required to promote p53 turnover, WT FAK or various FAK mutants (Figure 3A) were re-expressed via adenovirus (Ad) in low-passage FAK$^{-/-}$p21$^{-/-}$ fibroblasts, and steady-state p53 levels were determined after 48 hr by anti-p53 blotting (Figure 3B). Surprisingly, WT FAK and various FAK signaling mutants functioned equally to reduce p53 levels by 60%–90% compared to mock-transduced cells (Figure 3B). Overexpression of the FAK C-terminal domain

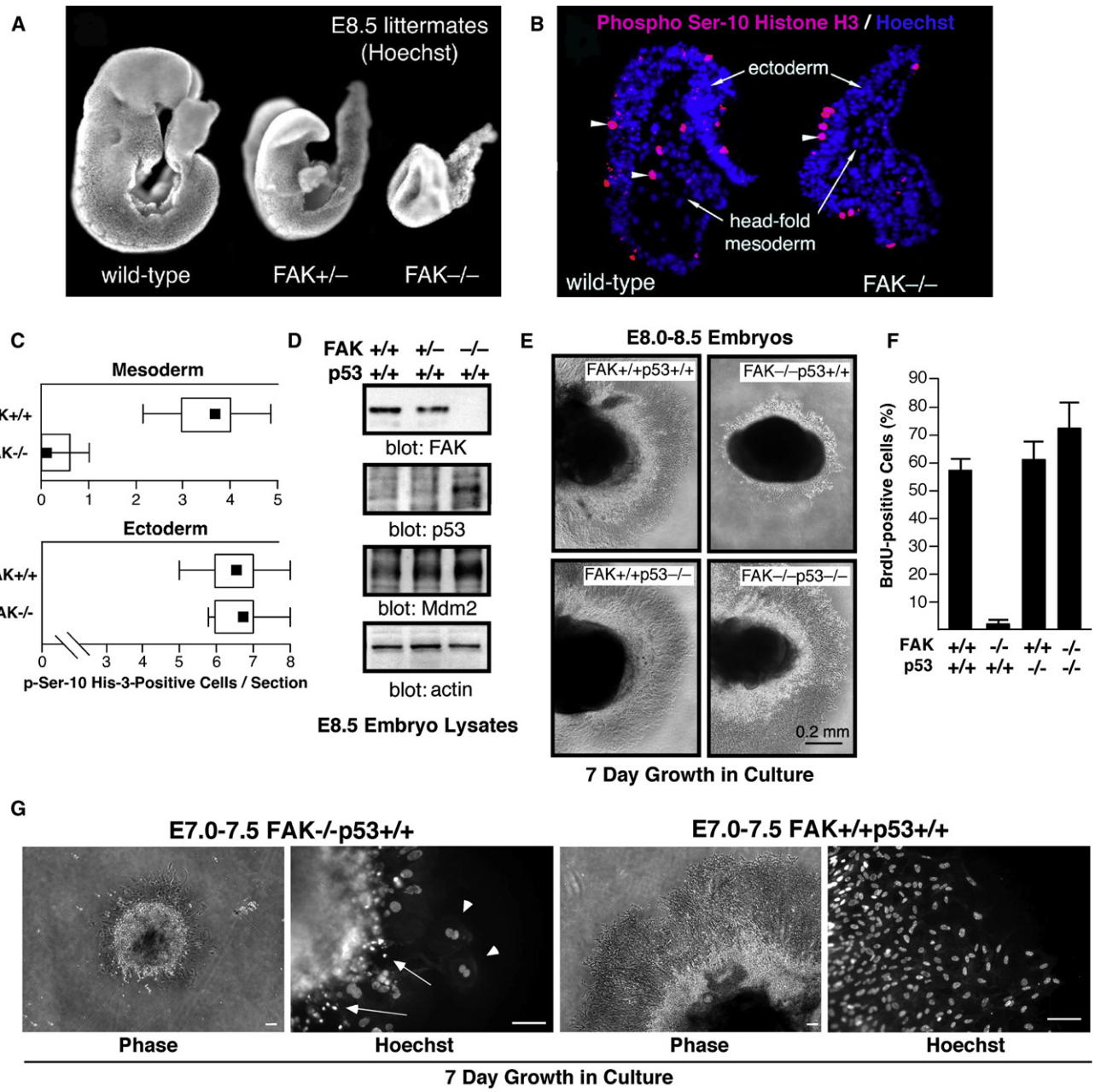

Figure 1. FAK$^{-/-}$ Embryo Mesoderm Cell Proliferation Block Is p53 Dependent

(A) Hoechst DNA staining of WT (FAK$^{+/+}$), FAK$^{+/-}$, and FAK embryos at E8.5.

(B) Mesoderm region of FAK$^{-/-}$ embryos lack mitotic cells. Sagittal head-fold sections of E8.0–8.5 FAK$^{+/+}$ and FAK$^{-/-}$ littermate embryos stained with phospho-serine-10 Histone H3 (red, arrowheads) and Hoechst (blue).

(C) Quantitation of phosphoserine-10 Histone H3 staining. Number of mitotic cells (per head-fold region section) in the ectoderm and mesoderm of FAK$^{-/-}$ and FAK$^{+/+}$ littermates plotted as box-and-whisker diagrams: dot (mean), box (25–75 percentile), and bars (minimum and maximum value).

(D) Immunoblotting of embryo lysates shows increased p53 and Mdm2 protein expression from E.8.5 FAK$^{-/-}$ compared to FAK$^{+/+}$ or FAK$^{+/-}$ littermates.

(E) p53 prevents FAK$^{-/-}$ embryo proliferation ex vivo. The indicated E8.0–8.5 embryos were dissected and cultured in Matrigel for 7 days. Phase contrast images are of Matrigel-embedded embryos (dark) and surrounding cells growing out from the embryo mass.

(F) Rescue of FAK$^{-/-}$ cell proliferation defects by p53 deletion. Percentage of BrdU-positive cells for the indicated genotype. Data are mean ± SEM from three independent experiments.

(G) E7.0–7.5 time of embryo extraction does not alter FAK$^{-/-}$p53$^{+/+}$ proliferation defects ex vivo. Phase images of embryos in Matrigel culture for 7 days (scale bar, 100 μm). Hoechst staining shows cells with multiple (arrowheads) and fragmented (arrows) nuclei in FAK$^{-/-}$p53$^{+/+}$ but not FAK$^{+/+}$p53$^{+/+}$ cultures.

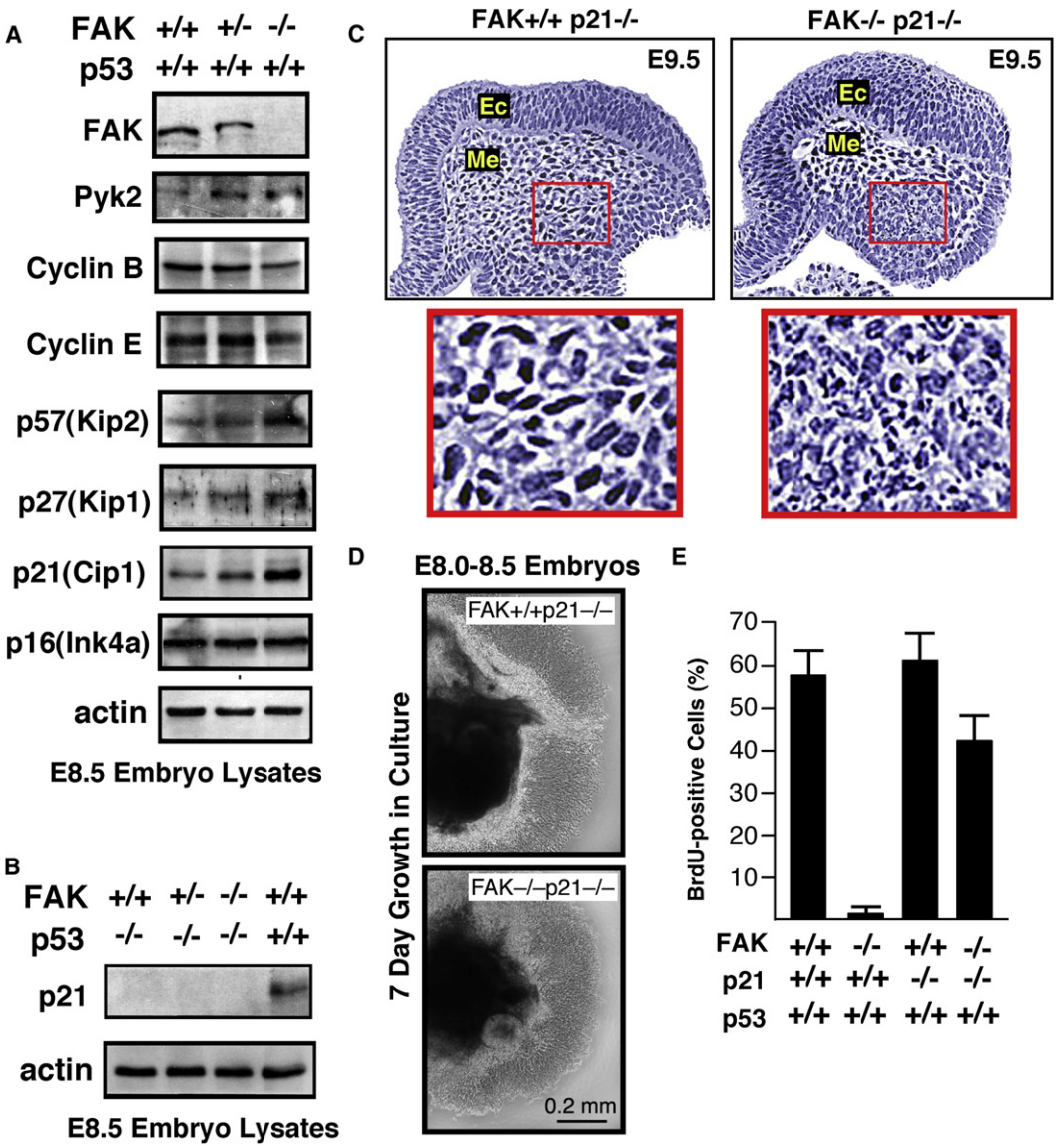

Figure 2. p53-Mediated Proliferation Block of FAK$^{-/-}$ Cells Is p21 Dependent

(A) Increased expression of p53, Pyk2, or cyclin-dependent kinase inhibitors and decreased expression of cyclins in FAK$^{-/-}$ compared to FAK$^{+/+}$ littermates as determined by immunoblotting of E8.5 embryo protein lysates.

(B) Lack of detectable p21 expression in lysates from FAK$^{-/-}$ E8.5 embryos on a p53$^{-/-}$ background.

(C) FAK$^{-/-}$p21$^{-/-}$ embryos exhibit lethality at E9.5. H&E staining of sagittal headfold sections. Ec, ectoderm; Me, mesoderm. (Inset) Fragmented nuclei observed in mesoderm region of FAK$^{-/-}$p21$^{-/-}$ but not FAK$^{+/+}$p21$^{-/-}$ embryos.

(D) E8.0–8.5 FAK$^{-/-}$p21$^{-/-}$ embryo cells proliferate equally to FAK$^{+/+}$p21$^{-/-}$ cells in 7 day Matrigel culture ex vivo. Phase contrast images of embryo mass (dark) and surrounding cells.

(E) p21 inactivation promotes FAK$^{-/-}$ embryo cell proliferation as determined by the percentage of BrdU-positive cells counted for the indicated genotype. Data are mean ± SEM from three independent experiments.

(termed FAK-related nonkinase, FRNK) slightly elevated p53 levels, whereas FAK residues 1–402 encompassing the FERM domain reduced p53 levels >80% (Figure 3B). As N-terminal truncated and activated FAK (Δ1–100) did not affect p53 levels and kinase-dead FAK decreased p53 levels (Figure 3B), our results support the notion that the FAK FERM domain plays a unique role in promoting p53 turnover in a kinase-independent manner.

p53 levels in cells are regulated by a balance between protein expression and degradation. Addition of MG132 proteasome inhibitor for 3 hr prior to cell lysis blocked FAK and FAK FERM effects on p53 (Figure 3C), supporting the conclusion that FAK FERM facilitates p53 turnover. To determine whether changes in p53 expression affect p53 transcriptional activity, a 2.4 kb region of the p21 promoter coupled to luciferase was used as a p53 activity reporter in FAK$^{-/-}$p21$^{-/-}$ cells (Figure 3D). High p53

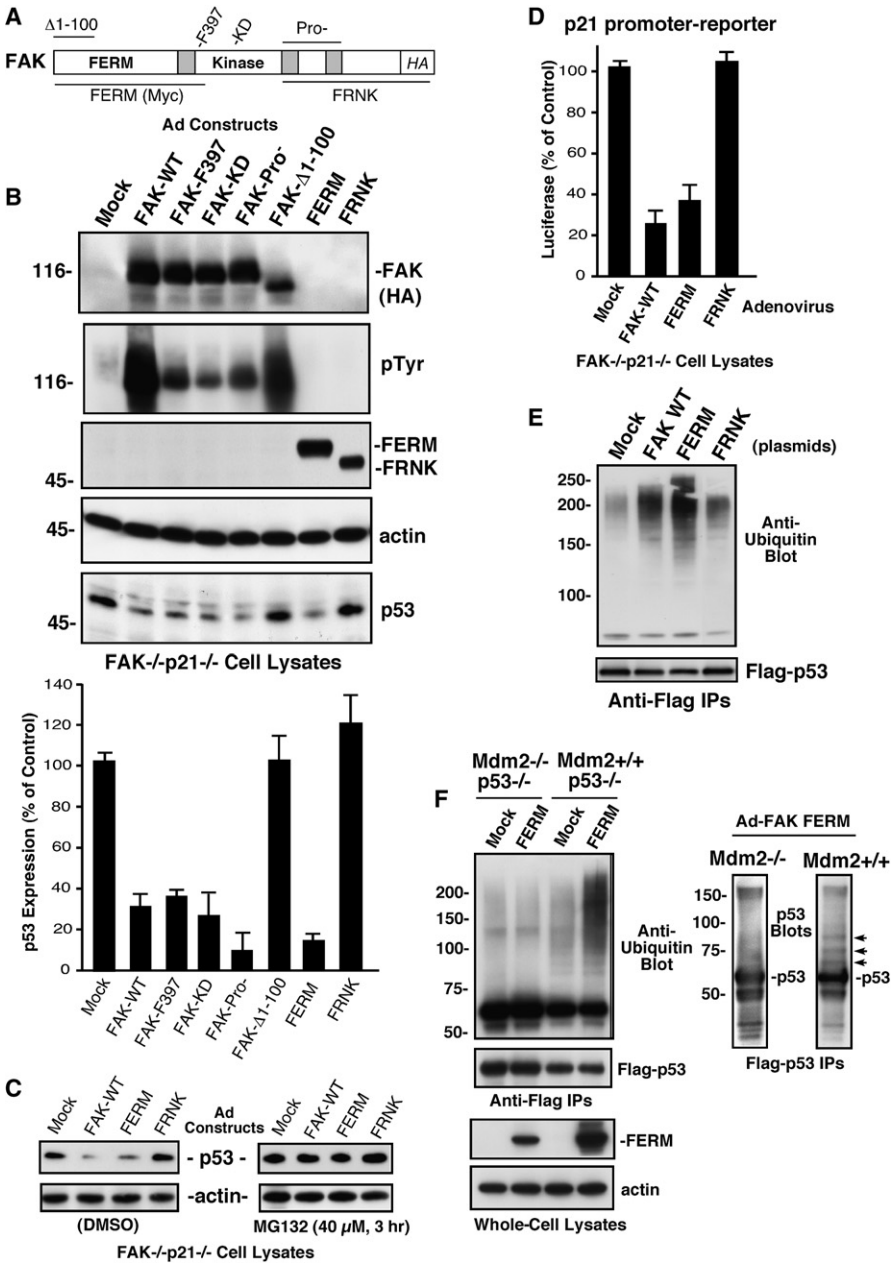

Figure 3. FAK FERM Inhibits p53 Activity through Enhanced Mdm2-Dependent Ubiquitination and Proteasomal Degradation

(A) Epitope-tagged FAK construct schematic. Indicated is the band 4.1, ezrin, radixin, moesin (FERM) and central kinase domains. Filled regions indicate proline-rich motifs. Translation of FAK Δ1–100 starts at Met-101; Myc-tagged FERM encompasses residues 1–402; and mutation of Y397 phosphorylation (F397), kinase-dead (KD, R454), Pro null (Pro 712, 713, 872, 873, 876, and 877 mutated to Ala), and FRNK residues 691–1052 are indicated.

(B) FAK FERM but not FAK kinase activity is required for the reduction of steady-state p53 levels in FAK$^{-/-}$p21$^{-/-}$ fibroblasts. Cells were transduced with Ad-Tet transactivator (TA, mock) or Ad-TA plus the indicated Ad-FAK, Ad-FERM, or Ad-FRNK constructs. After 48 hr, lysates were blotted with the indicated antibodies, p53 levels were quantified by densitometry, and mean values ± SD are expressed as percentage of control (mock) from two experiments.

(C) Addition of MG132 (40 μM, 3 hr) prior to cell lysis prevents Ad-FAK and Ad-FERM-mediated p53 degradation in FAK$^{-/-}$p21$^{-/-}$ fibroblasts.

(D) FAK and FERM, but not FRNK, inhibit p53 activity as measured by a p21 promoter luciferase assay in FAK$^{-/-}$p21$^{-/-}$ cells 48 hr after transfection. Values are means presented as percent of mock control ± SD from three experiments.

(E) FAK and FERM, but not FRNK, promote enhanced p53 ubiquitination. HEK293 cells were cotransfected with Flag-p53 and the indicated FAK constructs. MG132 was added 3 hr prior to lysis, and p53 was isolated by IP and analyzed by anti-ubiquitin and Flag-tag blotting.

(F) Mdm2 expression is required for FERM-enhanced p53 ubiquitination. Mdm2$^{-/-}$p53$^{-/-}$ or Mdm2$^{+/+}$p53$^{-/-}$ fibroblasts were transfected with Flag-p53 and then transduced with mock or Ad-FAK FERM. MG132 was added 3 hr prior to lysis, and p53 IPs were analyzed by anti-ubiquitin, anti-p53 (DO-1), and Flag-tag blotting. Anti-Myc blotting was used to detect FAK FERM and anti-actin for loading control. Arrows indicate p53-shifted bands induced by FERM expression in Mdm2$^{+/+}$ cells.

activity was detected in growing cells, and this was inhibited >3-fold by WT FAK and FAK FERM but not FRNK expression. MG132 addition prevented FAK and FAK FERM inhibition of p21 promoter activity (data not shown), and accordingly, full-length FAK and FAK FERM, but not FRNK, increased p53 ubiquitination (Figure 3E). To elucidate the ubiquitin E3 ligase for FAK FERM-mediated p53 modification, Flag-p53 was transfected in $Mdm2^{-/-}p53^{-/-}$ and $Mdm2^{+/+}p53^{-/-}$ fibroblasts. Elevated levels of ubiquitinated p53 and p53 band-shifts were detected upon Ad-FAK FERM overexpression only in $Mdm2^{+/+}$ cells (Figure 3F). These results show that FAK FERM promotes p53 turnover through enhanced Mdm2-associated p53 ubiquitination and degradation.

FAK FERM F2 Lobe Facilitates FAK Nuclear Localization

As activated p53 is primarily nuclear localized and exogenous FAK FERM is nuclear enriched (Golubovskaya et al., 2005; Stewart et al., 2002), analyses were undertaken to elucidate the determinants of FAK FERM nuclear targeting. Fusions of FAK residues (1–402) to green fluorescent protein (GFP) exhibit strong nuclear localization independent of Y397 phosphorylation (Figure S2A). The classic nuclear localization sequence typically contains clusters of basic amino acids. The avian FAK FERM domain is a three lobed (F1–F3) structure (Lietha et al., 2007). Primary sequence alignments of the murine FAK FERM F2 lobe region showed that FAK and Pyk2 contained patches of basic amino acids that are not conserved in other FERM-containing proteins such as ezrin, radixin, moesin, or merlin (Figure 4A). Although these FAK F2 FERM domain basic residues are separated by primary sequence, they comprise surface-exposed clusters (Figure 4B). The largest patch consists of residues K190, K191, K216, K218, R221, and K222, whereas a second smaller basic patch is comprised of R204, R205, and K209. Residues R177 and R178 are partially exposed within the FAK FERM F2 lobe structure (Figure 4B).

Alanine substitutions were introduced within the FAK FERM F2 lobe, and the effects on FAK FERM nuclear localization were monitored by fluorescence microscopy (data not shown) and cellular fractionation into nuclear (N) or cytosolic (C) extracts (Figure 4C). Mutations in the largest basic patch (K190/191A or K216/218A) blocked whereas mutations in a second smaller patch (K204/R205A) slightly reduced FERM nuclear accumulation. R177/R178A mutations also prevented FERM nuclear localization, whereas mutation of surface-exposed basic residues in the FAK FERM F3 lobe (R312/K313A) or the SUMOylation site (K152R) did not affect FERM nuclear targeting (Figure 4C). To prove the role of the FERM domain promoting FAK nuclear localization, GFP-FAK WT and GFP-FAK R177/R178A were expressed in $FAK^{-/-}$ fibroblasts or human umbilical endothelial cells (HUVECs) (data not shown) and GFP localization monitored by time-lapse imaging in the presence or absence of the nuclear export inhibitor leptomycin B (Figure 4D). In vehicle-treated cells, both FAK constructs were detected in focal contacts and the cytoplasm. Leptomycin B addition promoted WT but not FAK R177/R178A nuclear accumulation within 4 hr (Figure 4D).

To analyze whether endogenous FAK is present in the nucleus, nuclear (N) or cytosolic (C) HUVEC extracts were analyzed for FAK distribution (Figure 4E). Approximately 5%–10% of HUVEC FAK is nuclear associated and tyrosine phosphorylated. To determine whether cellular stress may enhance FAK nuclear accumulation, HUVECs were treated with the protein kinase inhibitor staurosporine (Figure 4F). Within 30 min, staurosporine enhanced endogenous FAK and GFP-FAK but not FERM F2 lobe-mutated GFP-FAK R177/178A nuclear accumulation. This was accompanied by FAK dephosphorylation, loss of FAK from focal contacts, and preceded staurosporine-induced HUVEC apoptosis occurring within 4–8 hr (Figures S2B–S2F). Staurosporine caused a rapid redistribution of GFP-FAK R177/178A from focal contacts to punctate cytoplasmic clusters, but not to the nucleus (Figure S2E). Loss of integrin-mediated cell adhesion is another cellular stressor, and this was also found to increase FAK nuclear accumulation within 30 min (Figure 4G). Together, these results support the importance of the FAK FERM F2 lobe in nuclear targeting. Moreover, the distribution of FAK at focal contacts, in the cytoplasm, or the nucleus is affected by cellular stress.

FAK Nuclear Localization Is Important for p53 Inhibition

Primary $FAK^{-/-}p21^{-/-}$ fibroblasts are a unique model system to determine the role of FAK in p53 regulation. Increased expression of the FAK-related Pyk2 kinase was detected in $FAK^{-/-}p21^{-/-}$ fibroblasts, and lentiviral-mediated Pyk2 shRNA was used to maintain low levels of Pyk2 for FAK re-expression studies (data not shown). To address whether FAK FERM nuclear localization is important for p53 regulation, stable pooled populations of GFP-FAK FERM (1–402) or GFP-FRNK-expressing $FAK^{-/-}p21^{-/-}$ fibroblasts were established. WT, K152R SUMOylation mutant, and R312/K313A FAK FERM F3 lobe-mutated proteins were nuclear localized, F2 lobe FERM mutants (R177/R178A and K190/K191A) were cytoplasmic distributed, and GFP-FRNK localized to focal contacts (Figure 5A and Table S2). Steady-state p53 levels in FAK FERM-expressing cells were evaluated by immunoblotting and compared to parental $FAK^{-/-}p21^{-/-}$ and GFP-expressing controls. Cells expressing WT FERM and the SUMOylation (K152R) FERM mutant exhibited reduced p53 levels (Figure 5B). Importantly, mutations in the FERM F2 lobe (K190/K191A and R177/R178A) blocked FAK FERM effects on lowering p53 levels (Figure 5B). However, mutations in the FAK FERM F3 lobe (R312/K313A) also blocked the ability of FAK FERM to reduce p53 levels (Figure 5B) even though R312/K313A FAK FERM was nuclear localized (Figure 5A). As p53 transcriptional activity paralleled p53 expression levels in FAK FERM-reconstituted $FAK^{-/-}p21^{-/-}$ fibroblasts (data not shown), the combined results support the notion that FAK FERM nuclear localization is required, but not sufficient, for p53 regulation.

To determine whether full-length FAK modulates p53 activity in a similar manner as the FAK FERM, cotransfection assays were performed in $FAK^{-/-}p53^{-/-}$ fibroblasts (Figure 5C). The p21 promoter-luciferase reporter was responsive to p53 re-expression resulting in ~14-fold increased activity. Coexpression of WT or SUMOylation mutant K152R FAK resulted in >65% inhibition of p53 activity, whereas equal expression of F2 lobe-mutated R177/R178A FAK lowered p53 activity only 5%–10% (Figure 5C). F2 lobe-mutated K190/K191A or F3 lobe-mutated R312/K313A FAK only weakly inhibited p53 activity. Taken together, these results support the conclusion that

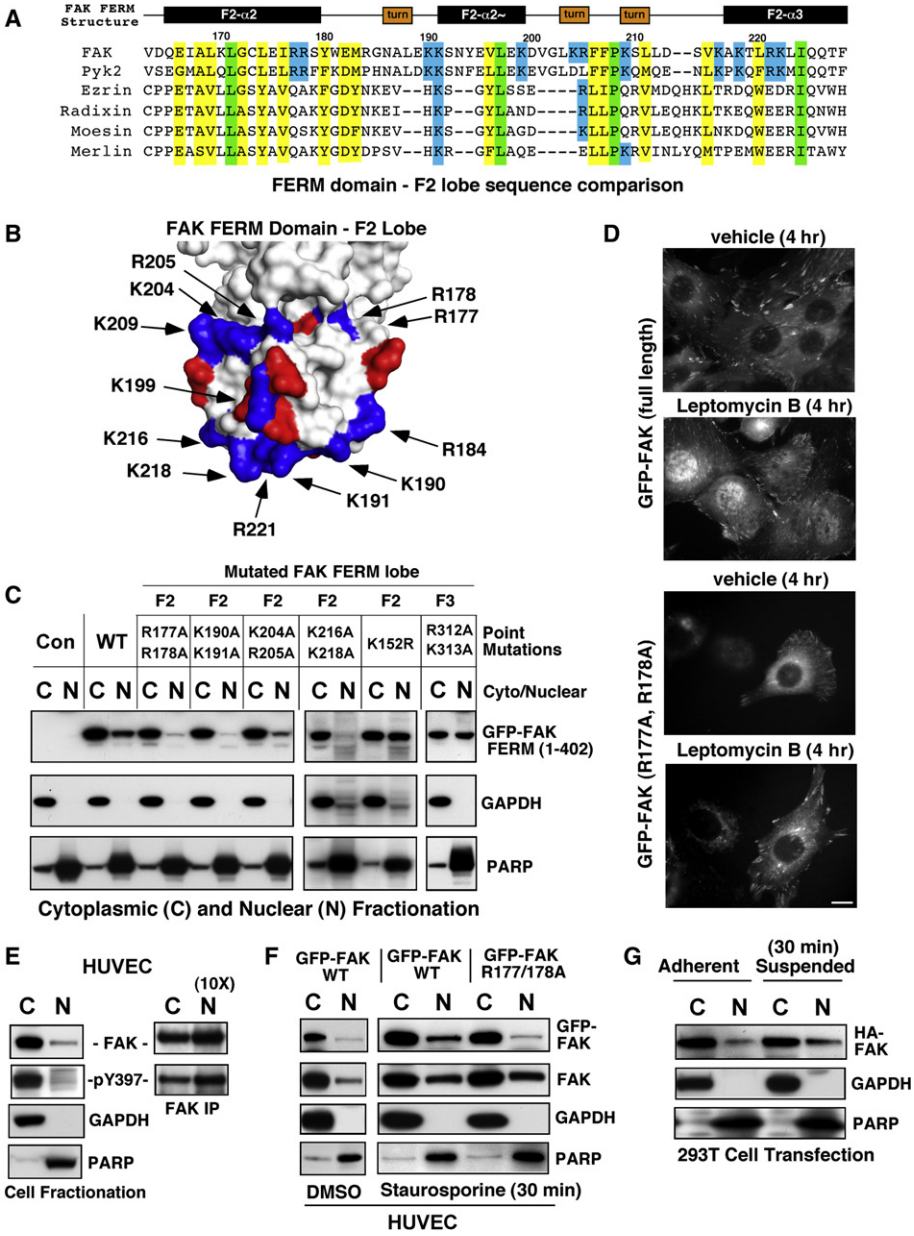

Figure 4. Determinants of FAK Nuclear Localization

(A) Structure-based alignment of FAK FERM F2 lobe residues (Lietha et al., 2007) with other FERM-containing proteins. Conserved basic residues within FAK and Pyk2 are highlighted in blue, total conserved FERM residues are highlighted in yellow, and identical residues are highlighted in green.

(B) Localization of basic residue clusters on the surface of the FAK FERM F2 lobe. The FAK FERM domain (Lietha et al., 2007) F2 lobe was visualized using MacPyMOL. Basic residues (blue) are numbered according to the primary FAK sequence, and acidic residues (red) are indicated. A putative nuclear targeting motif is comprised of residues at the tip of the F2 lobe (K190, K191, K216, K218, and R221).

(C) FAK FERM domain analyzed by cellular fractionation. The indicated residues within GFP-FAK FERM (1–402) were mutated and constructs expressed in 293T cells. Cell lysates were separated into cytosolic (C) and nuclear (N) fractions and resolved by SDS-PAGE, and anti-GFP blotting was used to detect FAK FERM. Antibodies to GAPDH and PARP were used to verify fractionation specificity, respectively.

(D) Live cell imaging was used to follow GFP-FAK WT and GFP-FAK R177/178A distribution upon leptomycin B (10 ng/ml) or ethanol (vehicle) addition for 4 hr. Scale bar, 10 μm.

(E) FAK is partially nuclear localized. HUVECs were separated into cytosolic and nuclear fractions and blotted for FAK, GAPDH, and PARP. Ten-fold excess nuclear lysates were used to analyze FAK tyrosine phosphorylation by IP.

(F) WT but not R177/178A FAK nuclear accumulation by HUVEC fractionation. HUVECs were treated with 1 μM staurosporine for 30 min and lysates separated into cytosolic or nuclear fractions and immunoblotted with antibodies to GFP, FAK, GAPDH, and PARP.

(G) 293T cells were transfected with HA-FAK and then fractionated into cytosolic and nuclear fractions under adherent and suspended conditions. Lysates blotted with anti-HA, GAPDH, and PARP.

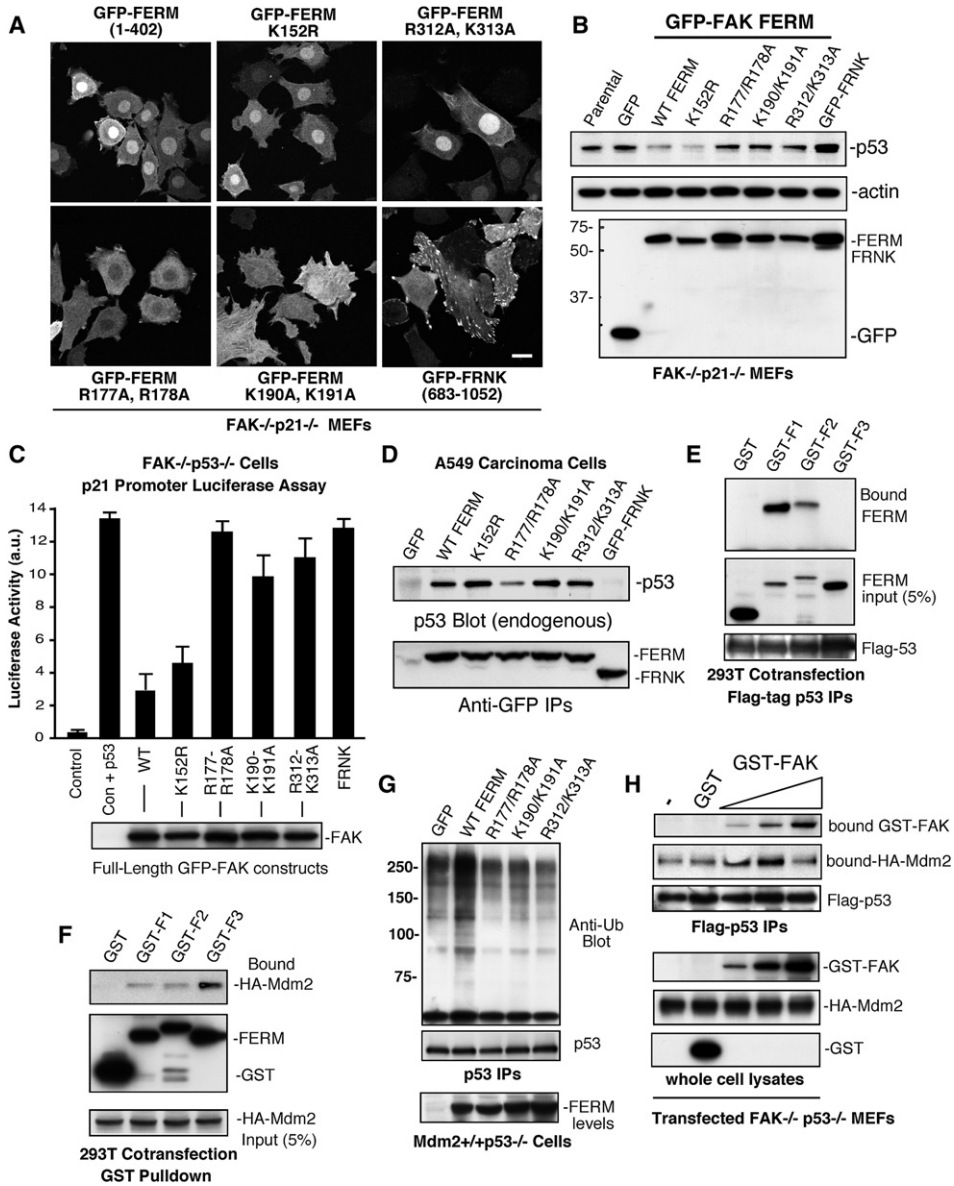

Figure 5. Separate FAK FERM Lobes Mediate p53 Binding, Nuclear Localization, and Mdm2 Association

(A) The indicated GFP-FAK FERM (1–402) constructs or GFP-FRNK were stably expressed in FAK$^{-/-}$p21$^{-/-}$ (Pyk2 shRNA) fibroblasts and intracellular distribution visualized by confocal microscopy. Scale bar, 20 μm.

(B) Steady-state p53 expression is reduced by FAK FERM expression in FAK$^{-/-}$p21$^{-/-}$ (Pyk2 shRNA) fibroblasts as detected by p53, actin, and GFP blotting of lysates.

(C) FERM domain mutations disrupt full-length FAK inhibition of p53 transcriptional activity. FAK$^{-/-}$p53$^{-/-}$ fibroblasts were transiently transfected with a 2.4 kb p21 promoter luciferase construct (Control, Con) or in combination with p53 (Vec+p53) and the indicated FAK constructs. Luciferase activity is arbitrary units (a.u.). Values are means of two experiments ± SD. Blotting verified equal FAK construct expression (below).

(D) F2 FERM mutations can weaken p53 association. Ad-FAK FERM or FRNK constructs were expressed in A549 cells and association with endogenous p53 analyzed by IP and blotting.

(E) FAK FERM F1 lobe binds p53. 293T cells were cotransfected with Flag-p53 and the indicated FAK F1, F2, or F3 FERM lobes as GST fusion proteins. Anti-GST blotting of Flag IPs was used to detect FERM lobe association with p53.

(F) FAK FERM F3 lobe binds Mdm2. 293T cells were cotransfected with HA-Mdm2 and the indicated FAK F1, F2, or F3 FERM lobes as GST fusion proteins. Cells were treated with MG132 prior to cell lysis (40 μM, 3 hr), incubated with glutathione agarose, and anti-HA blotting detected bound Mdm2.

(G) FAK FERM mutations disrupt FERM-enhanced p53 ubiquitination. Mdm2$^{+/+}$p53$^{-/-}$ fibroblasts were transfected with Flag-p53 and transduced with the indicated Ad-FAK FERM constructs, and MG132 was added 3 hr prior to lysis. p53 IPs were analyzed by anti-ubiquitin, Flag-tag, and GFP blotting.

(H) Biphasic FAK effects on Mdm2-p53 complex formation. HA-Mdm2 and Flag-p53 were transfected into FAK$^{-/-}$p53$^{-/-}$ fibroblasts, MG132 was added 3 hr prior to lysis, and GST (500 ng) or increasing amounts of recombinant GST-FAK (10–500 ng) were added prior to p53 isolation by IP. Bound Mdm2 and FAK within a p53 complex were detected by anti-HA and GST blotting.

FAK FERM F2 lobe-mediated nuclear translocation is important for p53 inhibition. However, the fact that FERM F3 lobe mutations (R312/K313A) did not affect nuclear translocation yet disrupted the ability of FAK to inhibit p53 indicates that FAK-mediated regulation of p53 involves multiple FERM-associated mechanisms.

FAK FERM Acts as a Scaffold to Facilitate p53 and Mdm2 Association

Coimmunoprecipitation (CoIP) analyses have shown that FAK and p53 can form a complex (Golubovskaya et al., 2005), but the binding determinants for p53 within the FAK FERM domain remain unknown. GFP-FAK FERM or GFP-FRNK constructs were expressed in human A549 cells and evaluated for endogenous p53 association by CoIP analyses (Figure 5D). p53 associated with FAK FERM, but not FRNK, and p53 binding to FAK FERM was weakened by mutations in the F2 (R177/R178A), but not F3 (R312/K313A), lobes (Figure 5D). Similar results were obtained by GST-p53 pull-down assays (Figure S3A). Interestingly, F2 lobe-mutated K190/K191A FAK FERM can form a complex with p53 (Figure 5D), but these FERM mutations disrupt nuclear localization (Figure 5A) and p53 regulation (Figures 5B and 5C). Additionally, F3 lobe-mutated R312/K313A FAK FERM localizes to the nucleus (Figure 5A) and binds to p53 (Figure 5D) but does not promote p53 turnover (Figure 5B). Together, these results support the notion that FERM-mediated nuclear localization, p53 binding, and FERM-enhanced p53 turnover are separable events.

To determine whether individual FAK FERM lobes can associate with p53 or Mdm2 in cells, the F1, F2, or F3 regions were transiently expressed as GST fusion proteins in 293T cells (Figures 5E and 5F). The FAK FERM F1 lobe strongly associated with p53 in vivo, whereas weak binding was detected with FAK FERM F2 lobe, and no p53 binding was detected with the FAK FERM F3 lobe (Figure 5E). This result supports the notion that the FAK FERM p53 binding site likely spans the F1 and F2 FERM lobe regions. For Mdm2, FAK FERM F3 lobe bound the strongest, with only weak interactions detected with F1 or F2 FAK FERM lobes (Figure 5F). Interestingly, F3 lobe-mutated R311/K312A FERM bound Mdm2, and surprisingly, F2 lobe-mutated R177/R178A FERM exhibited enhanced Mdm2 binding (Figure S3B). Cotransfection studies revealed that both F2 and F3 lobe FERM mutations disrupted FAK FERM-enhanced p53 ubiquitination (Figure 5G) and support the notion that FAK-enhanced p53 ubiquitination may be part of a nuclear-localized complex. Accordingly, although F2 lobe-mutated K190/K191 FERM can bind p53, this mutant is cytoplasmic distributed and fails to promote p53 ubiquitination. For F3 lobe-mutated R312/K313A FERM, it is likely that this mutation disrupts the binding of another protein other than Mdm2 that is needed to facilitate p53 ubiquitination.

To support the notion that FAK may act as a scaffold to enhance the formation of a p53-Mdm2 complex, $FAK^{-/-}p53^{-/-}$ fibroblasts were transfected with Flag-p53, HA-Mdm2, and increasing amounts of recombinant GST or GST-FAK added to cell lysates. A p53-Mdm2 association was detected in the absence of FAK, and this was not affected by purified GST addition (Figure 5H). GST-FAK addition increased the amount of p53-bound Mdm2 through the formation of a p53-Mdm2-FAK complex in a dose-dependent manner. However, excess GST-FAK did not enhance p53-Mdm2 complex formation even though increased GST-FAK bound to p53 (Figure 5H). This result is consistent with a biphasic scaffolding effect of FAK in facilitating p53 and Mdm2 interactions. Together with the FERM mutational results, these studies support the conclusion that nuclear-localized FAK functions as a FERM-associated scaffold for p53 and Mdm2 binding that facilitates p53 ubiquitination leading to p53 turnover.

FAK Regulation of Cell Proliferation and p53-Dependent Apoptosis in Human Fibroblasts

As our studies support the importance of FAK in regulating p53 activation during development and in mouse fibroblasts, lentiviral-mediated FAK shRNA knockdown was used to test whether a FAK-p53 signaling axis exists in human fibroblasts and HUVECs. Within 72 hr, >80% of cells showed strong lentiviral GFP expression, and neither anti-FAK nor scrambled (Scr) shRNA expression promoted cell apoptosis (Figure S4). However, >75% reduction in FAK expression was associated with ~2-fold increased p53-p21 protein levels and reduced cell proliferation (Figures 6A and 6B and Figure S5). To determine whether decreased FAK and elevated p53 levels would sensitize cells to DNA-damaging agents, Scr and FAK shRNA-expressing fibroblasts were treated with cisplatin. FAK shRNA cells showed ~4-fold increased apoptosis compared to cisplatin-treated Scr shRNA cells (Figures 6C and 6D) and the combination FAK shRNA plus cisplatin led to elevated p53 protein levels compared to cisplatin-treated Scr shRNA fibroblasts (Figure 6E).

To verify that increased cisplatin-stimulated apoptosis was due to decreased FAK, human fibroblasts were treated with FAK shRNA, and after 48 hr, cells were transduced with murine Ad-FAK WT or Ad-FAK Δ1–100 containing a deletion in the FAK FERM domain (Figures 6F and 6G). This truncation of FAK activates FAK kinase activity and facilitates FAK signaling (Mitra and Schlaepfer, 2006), but FAK Δ1–100 does not function to regulate p53 levels in mouse fibroblasts (Figure 3B). WT FAK re-expression blocked cisplatin-stimulated apoptosis in FAK shRNA cells, whereas Δ1–100 FAK had no effect (Figure 6F). Importantly, Δ1–100 FAK exhibited high activity levels as determined by antiphosphotyrosine blotting of fibroblast lysates and led to the robust activation of survival-associated signaling pathways such as Akt (Figure 6G). However, only WT FAK reduced p53 levels and prevented p21 expression in cisplatin-treated cells (Figure 6G). Importantly, cisplatin-stimulated apoptosis in FAK shRNA-expressing fibroblasts was dependent upon p53 as siRNA-mediated p53 reduction blocked both increased p21 expression and cell death (Figures 6H and 6I).

To prove the importance of the FAK FERM domain function in preventing cisplatin-stimulated apoptosis, cell survival analyses were performed after Ad-FERM WT or Ad-FERM R177/R178A expression in FAK shRNA knockdown human fibroblasts (Figures 6J and 6K). FAK FERM, but not R177/178A FERM, blocked p53 accumulation, and only WT FAK FERM functioned to prevent apoptosis. These results are strong support for the biological importance of the FAK FERM domain in the regulation of p53-dependent cell survival.

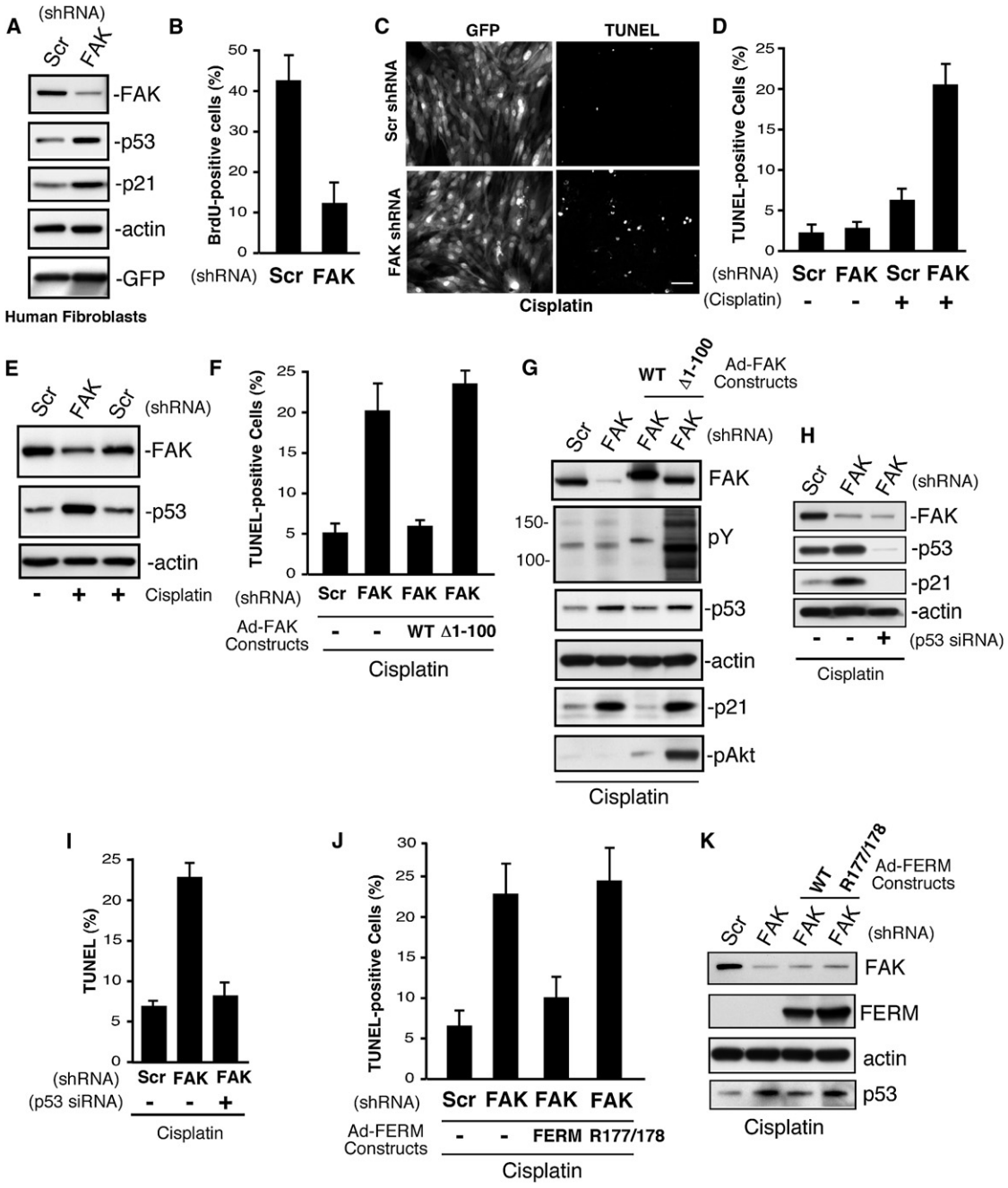

Figure 6. FAK Controls Human Diploid Fibroblast Proliferation and p53-Dependent Apoptosis

(A) Lysates from scrambled (Scr) and FAK shRNA infected cells after 72 hr were analyzed by anti-FAK, p53, p21, actin, and GFP blotting.

(B) FAK shRNA inhibits human fibroblast proliferation. Cells were infected with the indicated lentivirus for 72 hr, BrdU was added for 16 hr in growth media, and cells stained with anti-BrdU antibody. Mean values ± SD are percent of total GFP-positive cells.

(C and D) FAK shRNA sensitizes human fibroblasts to cisplatin-stimulated apoptosis. Cells were infected with the indicated lentivirus for 48 hr, cisplatin (20 μg/ml) was added for 48 hr, and cells were fixed and then analyzed by TUNEL staining. (C) Representative images of GFP-expressing and TUNEL-stained fibroblasts. Scale bar, 200 μm. (D) Mean values ± SD for cisplatin-stimulated apoptosis were obtained by counting three TUNEL-stained 10× fields of cells from two coverslips. Only GFP-positive cells were counted, and the data represent two independent experiments.

(E) Elevated p53 levels in cisplatin-treated FAK shRNA-expressing fibroblasts as treated as in (D) and analyzed by anti-FAK, p53, and actin blotting.

(F and G) FERM domain integrity is required for rescue of cisplatin-stimulated apoptosis. Cells were infected with Scr or FAK shRNA lentivirus (48 hr), transducted with Ad-FAK or Ad-FAK (Δ1–100), and after 24 hr, cisplatin (20 μg/ml, 48 hr) was added prior to analysis by TUNEL staining. (F) Mean values ± SD for cisplatin-stimulated apoptosis were obtained as described for (D). (G) FAK, but not Δ1–100 FAK, reverses cisplatin-stimulated increases in p53 and p21 expression as determined by blotting. Δ1–100 FAK activates Akt as determined by phospho-specific blotting.

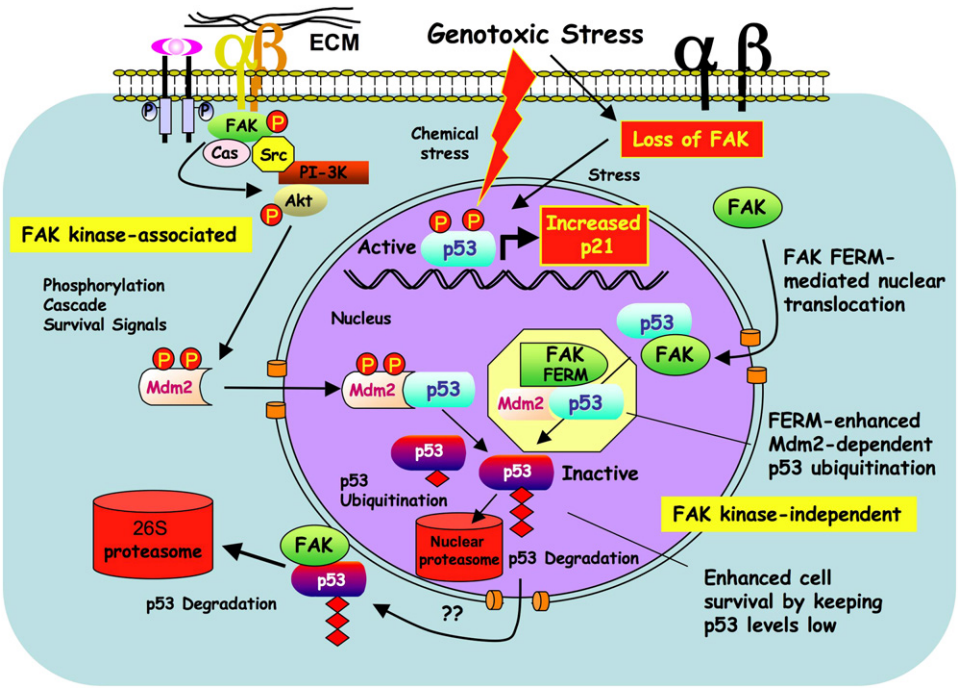

Figure 7. Model of FAK FERM-Mediated p53 Turnover and Cell Survival

FAK can function with integrins and growth factor receptors to promote cell survival through signaling cascades such as Akt that can activate ubiquitin E3-ligases such as Mdm2 to maintain low p53 levels. This canonical survival pathway involves FAK kinase activity (left). Under reduced integrin adhesion or conditions of cellular stress, FAK leaves focal contacts sites. This increases the cytoplasmic pool of FAK and enhances FAK nuclear accumulation via FAK-FERM-mediated targeting. Nuclear FAK acts as a scaffold to stabilize a p53-Mdm2 complex, leading to p53 polyubiquitination and subsequent p53 degradation by nuclear or cytoplasmic proteasomes. This regulatory connection between FAK and p53 is dependent on the FAK FERM domain but does not require FAK kinase activity (right).

DISCUSSION

Null mutation of FAK results in an early embryonic lethal phenotype (Ilic et al., 1995). Here, we show that *fak* inactivation is associated with the cessation of mesodermal cell proliferation and p53 activation during development. Interestingly, FAK null embryo ectoderm did not exhibit growth defects in vivo, and this may be due to different regulatory signals in epithelial versus mesodermal cells. However, as FAK null primary keratinocytes can proliferate in culture (Schober et al., 2007), cells of ectodermal origin may have different or compensatory survival mechanisms compared to mesodermal fibroblasts. Interestingly, genetic inactivation of p53 or p21 in FAK null embryos did not rescue the embryonic lethal phenotype that remains associated with altered morphogenesis (Ilic et al., 1995). However, loss of p53 or p21 enabled $FAK^{-/-}$ embryo cell proliferation ex vivo. Thus, p53 activation induces cell-cycle arrest through p21 when FAK expression is impaired.

Unlike FAK, loss of other integrin-associated signaling proteins such as Src, p130Cas, paxillin, talin, or vinculin does not result in p53 activation or the blockage of primary fibroblast proliferation. Thus, FAK regulation of p53 during development is unlikely to involve canonical integrin signaling connections (Figure 7). Moreover, FAK connections to p53 are conserved in primary human cells as FAK shRNA knockdown promotes increased p53/p21 levels accompanied by decreased cell proliferation. Interestingly, conditional inactivation of FAK in endothelial (Braren et al., 2006; Shen et al., 2005) or Schwann cells (Grove et al., 2007) is linked to apoptosis or decreased cell proliferation, respectively. This may be associated with p53 activation as primary $FAK^{-/-}$ endothelial cell proliferation was facilitated by p53 inactivation (Ilic et al., 2003).

FAK FERM Survival Pathway

Strikingly, we found that FAK catalytic activity was not required for FAK-mediated regulation of p53. Although FAK

(H and I) FAK shRNA-enhanced cisplatin-stimulated apoptosis is p53 dependent. Fibroblasts were transfected with p53 siRNA, transduced with Scr or FAK shRNA lentivirus, and treated with cisplatin (20 μg/ml, 48 hr). (H) Blotting for FAK, p53, and p21 blotting shows changes in protein expression with actin blotting as control. (I) Mean values ± SD for cisplatin-stimulated apoptosis were obtained as for (D).

(J and K) FAK FERM domain rescue of cisplatin-stimulated apoptosis. Cells were transduced with Scr or FAK shRNA lentivirus (48 hr), infected with Ad-Myc-FERM WT or Ad-Myc-FERM R177/R178 (24 hr), and then treated with cisplatin (20 μg/ml, 48 hr). (J) Cells were analyzed for TUNEL staining as in (D). (K) Blotting for FAK, Myc tag (FERM), actin, and p53 shows that FERM mutation blocks p53 regulation.

kinase-associated signals have been shown to repress p21 expression (Bryant et al., 2006; Ding et al., 2005), we found that kinase-inactive FAK functioned equally to WT FAK in repressing p53 expression using $FAK^{-/-}p21^{-/-}$ MEFs. Moreover, under stress induced by FAK knockdown combined with cisplatin addition to trigger p53 activation, re-expression of WT but not truncated (Δ1–100) FAK repressed p53/p21 expression and prevented p53-mediated apoptosis in human fibroblasts. Notably, Δ1–100 FAK was highly active and facilitated signals leading to Akt phosphorylation but did not function to promote survival. The inability of Δ1–100 FAK to counteract p53 activation is associated with the disruption of FERM domain function, as exogenous FAK FERM re-expression was sufficient to prevent cisplatin-stimulated apoptosis under FAK knockdown conditions.

To date, many studies have focused on the role of FAK kinase-associated cell survival pathways indirectly through dominant-negative type experiments (Reddig and Juliano, 2005). However, as a small molecule FAK catalytic inhibitor did not effect either normal or carcinoma cell proliferation or survival in culture (Slack-Davis et al., 2007), these overexpression studies may need to be re-evaluated. As FAK functions as both a scaffold and signaling kinase, it is also difficult to distinguish the survival and proliferation alterations caused by the loss of FAK expression. Using a strategy of FAK re-expression within $FAK^{-/-}$ or FAK knockdown fibroblasts, our studies have identified the FAK FERM domain as the key module of a kinase-independent FAK-p53 regulatory cell survival circuit. Previously, FAK FERM domain overexpression has been shown to suppress apoptotic stimuli via interactions with the death domain kinase receptor-interacting protein (Kurenova et al., 2004) and indirectly implicated in the transcriptional inhibition of p53 via binding to the p53 transactivation domain (Golubovskaya et al., 2005). Our studies support a different mode of p53 inhibition by FAK as proteasomal inhibitors prevent FAK inhibition of p53. We show that FAK inhibits p53 via FAK FERM nuclear translocation, FERM-mediated binding to p53, and FERM-enhanced Mdm2-dependent p53 ubiquitination (Figure 7).

Nuclear FAK, p53 Binding, and FERM-Enhanced p53 Degradation

The FAK FERM domain is comprised of three lobes (F1–F3) with similarity to other known FERM structures despite low primary sequence conservation (Lietha et al., 2007). Through mutagenesis, biochemical cell fractionation, and confocal microscopy, we identified a patch of basic residues as a nuclear localization motif within the FAK FERM F2 lobe (K190, K191, K216, K218, and R221). These basic residues are separated by primary sequence, conserved between FAK and Pyk2, and not present in other FERM domain-containing proteins. As other F2 lobe (R177/R178A), but not F3 lobe (R312/K313A), FAK FERM mutations also disrupt FAK nuclear localization, correct F2 lobe FERM folding is also likely important for FAK nuclear targeting.

Coimmunoprecipitation analyses using the individual FAK FERM lobes revealed that the F1 lobe bound strongest to p53, whereas the F3 lobe bound to Mdm2 independent of p53 association. Overall, p53 inactivation by FAK required FAK FERM F1 lobe binding to p53, FERM F2 lobe-mediated nuclear localization, and FERM F3 lobe for connections to Mdm2 and proteasomal degradation. Importantly, mutations in the FERM F2 lobe (K190/K191A and R177/R178A) and within the FAK FERM F3 lobe (R312/K313A) blocked the ability of FAK FERM to reduce p53 levels. The mechanism or mechanisms associated with these mutational effects are likely distinct. F2 lobe R177/R178A and K190/K191A FERM mutants can weakly bind p53, but they are cytoplasmically distributed and do not promote p53 ubiquitination. Even though F3 lobe-mutated R312/K313A FAK FERM was nuclear localized and can bind Mdm2, this mutation also disrupts the ability of FAK FERM to facilitate p53 ubiquitination. As FAK forms a multiprotein scaffolding complex with p53 and Mdm2 in a biphasic manner, we speculate that the presence of FAK in the nucleus acts to stabilize a p53-Mdm2 complex, leading to p53 polyubiquitination, and subsequent p53 degradation by nuclear or cytoplasmic proteasomes.

What conditions may promote FAK translocation to the nucleus? The nuclear export inhibitor leptomycin B promoted FAK nuclear accumulation in hours, whereas staurosporine treatment or loss of cell adhesion enhanced FAK nuclear distribution within 30 min. Nuclear FAK accumulation was also associated with a loss of FAK at focal contacts, and this supports the notion that there is a cytoplasmic pool of FAK that is free to shuttle in and out of the nucleus. We propose a model whereby, under conditions of cellular stress or reduced integrin signaling, the cytoplasmic pool of FAK is elevated, leading to increased FAK nuclear accumulation, which acts to enhance cell survival by facilitating p53 turnover. At present, the signals that regulate FAK cytoplasmic to nuclear movement remain undetermined. Although SUMOylated FAK was nuclear enriched (Kadare et al., 2003), we found that K152 FAK SUMOylation was not essential for nuclear translocation. Interestingly, some transformed cell types can survive under suspension conditions, and this associated with reduced p53 activation (Lewis et al., 2002). As FAK levels are elevated in many tumor cells (McLean et al., 2005), and we find that FAK can form a complex with p53 in both normal and tumor cells, future studies will be aimed at determining whether this FAK-p53 cell survival pathway may also play a role in promoting tumor progression.

EXPERIMENTAL PROCEDURES

Mice

$p53^{-/-}$, $p21^{-/-}$, and heterozygous FAK mice were housed and bred according to AALAC-approved institutional guidelines. Genomic DNA from placental cone and yolk sac were used for genotyping by PCR as described (Deng et al., 1995; Furuta et al., 1995; Tsukada et al., 1993). Littermates from crossings of $FAK^{+/-}$ mice were dissected at E7.5 or E8.5, fixed briefly in 3.8% paraformaldehyde for 20 min, and embedded in OCT. Sections (5 μm) were stained with anti-phosphoserine-10 Histone3 (Upstate Biotech) and Hoechst 33342 (10 μg/ml, Molecular Probes) to identify proliferating cells.

Embryo Explant Culture

E7.5–8.5 embryos were dissected from yolk sac and fetal membranes, placed in a drop of Matrigel (BD Biosciences), and cultured for 7 days in 10% FBS DMEM supplemented with 10^{-4} M β-mercaptoethanol. To determine cell proliferation ex vivo, 10 μM BrdU was added to day 6 embryo explants. After 24 hr, embryos were disaggregated using trypsin and cells were plated in 10 μg/ml fibronectin-coated wells (Roche) in complete medium containing 10 μM BrdU for an additional 24 hr. Cells were fixed and stained with FITC-labeled anti-BrdU antibody (Roche), and Hoechst 33342 (10 μg/ml) was added

as a DNA counterstain. Data represent a minimum of five litters from mating of FAK-heterozygous mice on various genetic backgrounds.

Cells

$FAK^{-/-}p53^{-/-}$ and mouse embryonic fibroblasts (MEFs) were generated as described (Ilic et al., 1995). $FAK^{-/-}p21^{-/-}$ and $FAK^{+/+}p21^{-/-}$ MEFs were from E8.0 embryos and maintained on dishes precoated with 0.1% gelatin up to 15 passages. $Mdm2^{-/-}p53^{-/-}$ MEFs were provided by S. Jones (University of Massachusetts Medical School). Human diploid foreskin BJ fibroblast and A549 lung carcinoma cells were obtained from ATCC. BJ fibroblast passage was limited to 50 doublings. Pyk2 shRNA-expressing $FAK^{-/-}p21^{-/-}$ cells were generated by lentiviral infection and sorting for GFP. Lentiviral-associated GFP expression was removed by Ad-Cre transduction and verified by flow cytometry. Primary HUVECs were from Glycotech (Gaithersburg, MD).

Immunoblotting, Antibodies, and Chemicals

E8.5 embryos were dissected from yolk sac and fetal membranes and then snap frozen. Five to ten embryos from three or more pregnant females were pooled together for each analysis. Embryos or cell lysates were made using modified RIPA buffer as described (Mitra et al., 2006). Anti-FAK (4.47) and phosphotyrosine (4G10), Cyclin B1 (clone V152), and Cyclin E (07-687) were from Millipore. Mouse anti-HA (16B12), Myc-tag (9E10), and GFP (B34) were from Covance Research, and rat anti-HA tag (clone 3F10) was from Roche. Anti-β-actin (AC-17) and Flag-tag (M4) were from Sigma. Anti-Mdm2 (SMP-14), p21 (F-5), $p16^{Ink4a}$ (F-12), $p57^{Kip2}$ (H-91), and p53 (DO-1) were from Santa Cruz. Anti-Pyk2 (clone 11), PARP (clone 42), and $p27^{Kip1}$ (clone 57) were from BD-Transduction. Anti-GAPDH (374, Chemicon), p53 (PAb240 and PAb122, Invitrogen), ubiquitin (FK-2, Biomol), pAkt (Ser-473, Cell Signaling Technology), and GST (30001, Pierce) were purchased. Anti-human p53 (CM1) and mouse p53 (CM5) were from Novocasta. Rabbit polyclonal anti-GFP was raised against recombinant 6-His-tagged-GFP produced from baculovirus culture. Affinity-purified anti-GFP antibodies were used for GFP-FAK FERM immunoprecipitation studies. ImageJ (1.36b) was used for densitometry and measurement of pixel intensity. Purified GST-FAK was from Active Motif. MG132, cisplatin, and staurosporine were from Calbiochem, and Leptomycin B was from LC Laboratories.

FAK Nuclear Localization and Subcellular Fractionation

$FAK^{-/-}p21^{-/-}$ MEFs expressing GFP-FAK FERM constructs were grown on glass coverslips coated with 0.1% gelatin, washed, fixed in 3.7% paraformaldehyde, and visualized by confocal microscopy (Bio-Rad Radiance 2100). $FAK^{-/-}p53^{-/-}$ MEFs expressing GFP-FAK WT or GFP-FAK R177/R178A mutants were grown on gelatin-coated glass coverslips in the presence or absence of leptomycin B (10 ng/ml) for 4 hr, fixed in 3.7% paraformaldehyde, and visualized at 60× using an inverted microscope (Olympus). Cellular fractionation studies were performed on transfected 293T cells and HUVECs in the absence or the presence of 1 μM staurosporine. After 48 hr, cells were washed in cold PBS and lysed with Cyt buffer (10 mM Tris [pH 7.5], 0.05% NP-40, 3 mM $MgCl_2$, 100 mM NaCl, 1 mM EGTA, 20 μg/ml aprotinin, 1 mM orthovanadate, and 10 μg/ml leupeptin). Cells were scrape loaded into tubes, incubated for 5 min at 4°C, spun at 800 × g at 4°C (5 min), and cytosolic supernatants collected. Cell pellets were further washed with cyto buffer twice to remove residual cytosolic proteins. Purified nuclei were resuspended in RIPA buffer, spun at 16,000 × g for 15 min, and supernatant collected as the nuclear fraction. Samples were separated by SDS-PAGE and immunoblotted for gylceraldehyde-3-phosphate dehydrogenase (GAPDH) and poly ADP-ribose polymerase (PARP) as cytoplasmic and nuclear markers, respectively.

Supplemental Data

Supplemental Data include Supplemental Experimental Procedures, Supplemental References, two tables, and five figures and can be found with this article online at http://www.molecule.org/cgi/content/full/29/1/9/DC1/.

ACKNOWLEDGMENTS

We thank P. Leder (Harvard University) for $p21^{-/-}$ mice and S. Aizawa (RIKEN, Japan) for $p53^{-/-}$ mice. We are indebted to C. Kannemeier (Scripps), E. Choi (Scripps), and the Scripps Flow facility for technical help. We appreciate this assistance of V. Ossovskaya (University of California, San Francisco [UCSF]) and P. Sun (Scripps) for discussions and C. Damsky (UCSF) for critical review. Part of these studies was conducted in a facility constructed with support from the Research Facilities Improvement Program (C06RR16490). Y.L. was support in part by a Korean Research Foundation Grant (M01-2005-000-10071). D.I. was supported by grant CA87652. D.D.S. is an American Heart Association Established Investigator (0540115N) and is supported by grants CA87038, CA75240, and CA102310 from the National Institutes of Health. None of the authors have a financial interest related to this work.

Received: April 6, 2007
Revised: July 31, 2007
Accepted: November 16, 2007
Published: January 17, 2008

REFERENCES

Bao, W., Thullberg, M., Zhang, H., Onischenko, A., and Stromblad, S. (2002). Cell attachment to the extracellular matrix induces proteasomal degradation of p21(CIP1) via Cdc42/Rac1 signaling. Mol. Cell. Biol. *22*, 4587–4597.

Braren, R., Hu, H., Kim, Y.H., Beggs, H.E., Reichardt, L.F., and Wang, R. (2006). Endothelial FAK is essential for vascular network stability, cell survival, and lamellipodial formation. J. Cell Biol. *172*, 151–162.

Bryant, P., Zheng, Q., and Pumiglia, K. (2006). Focal adhesion kinase controls cellular levels of p27/Kip1 and p21/Cip1 through Skp2-dependent and -independent mechanisms. Mol. Cell. Biol. *26*, 4201–4213.

Cohen, L.A., and Guan, J.L. (2005). Residues within the first subdomain of the FERM-like domain in focal adhesion kinase are important in its regulation. J. Biol. Chem. *280*, 8197–8207.

Cox, B.D., Natarajan, M., Stettner, M.R., and Gladson, C.L. (2006). New concepts regarding focal adhesion kinase promotion of cell migration and proliferation. J. Cell. Biochem. *99*, 35–52.

Deng, C., Zhang, P., Harper, J.W., Elledge, S.J., and Leder, P. (1995). Mice lacking p21CIP1/WAF1 undergo normal development, but are defective in G1 checkpoint control. Cell *82*, 675–684.

Ding, Q., Grammer, J.R., Nelson, M.A., Guan, J.L., Stewart, J.E., Jr., and Gladson, C.L. (2005). p27Kip1 and cyclin D1 are necessary for focal adhesion kinase regulation of cell cycle progression in glioblastoma cells propagated in vitro and in vivo in the scid mouse brain. J. Biol. Chem. *280*, 6802–6815.

Furuta, Y., Ilic, D., Kanazawa, S., Takeda, N., Yamamoto, T., and Aizawa, S. (1995). Mesodermal defect in late phase of gastrulation by a targeted mutation of focal adhesion kinase, FAK. Oncogene *11*, 1989–1995.

Gilmore, A.P. (2005). Anoikis. Cell Death Differ. *12* (*Suppl 2*), 1473–1477.

Golubovskaya, V.M., Finch, R., and Cance, W.G. (2005). Direct interaction of the N-terminal domain of focal adhesion kinase with the N-terminal transactivation domain of p53. J. Biol. Chem. *280*, 25008–25021.

Gottlieb, E., Haffner, R., King, A., Asher, G., Gruss, P., Lonai, P., and Oren, M. (1997). Transgenic mouse model for studying the transcriptional activity of the p53 protein: age- and tissue-dependent changes in radiation-induced activation during embryogenesis. EMBO J. *16*, 1381–1390.

Grove, M., Komiyama, N.H., Nave, K.A., Grant, S.G., Sherman, D.L., and Brophy, P.J. (2007). FAK is required for axonal sorting by Schwann cells. J. Cell Biol. *176*, 277–282.

Harris, S.L., and Levine, A.J. (2005). The p53 pathway: positive and negative feedback loops. Oncogene *24*, 2899–2908.

Ilic, D., Furuta, Y., Kanazawa, S., Takeda, N., Sobue, K., Nakatsuji, N., Nomura, S., Fujimoto, J., Okada, M., Yamamoto, T., and Aizawa, S. (1995). Reduced cell motility and enhanced focal adhesion contact formation in cells from FAK-deficient mice. Nature *377*, 539–544.

Ilic, D., Almeida, E.A., Schlaepfer, D.D., Dazin, P., Aizawa, S., and Damsky, C.H. (1998). Extracellular matrix survival signals transduced by focal adhesion kinase suppress p53-mediated apoptosis. J. Cell Biol. *143*, 547–560.

Ilic, D., Kovacic, B., McDonagh, S., Jin, F., Baumbusch, C., Gardner, D.G., and Damsky, C.H. (2003). Focal adhesion kinase is required for blood vessel-morphogenesis. Circ. Res. *92*, 300–307.

Iwakuma, T., and Lozano, G. (2003). MDM2, an introduction. Mol. Cancer Res. *1*, 993–1000.

Kadare, G., Toutant, M., Formstecher, E., Corvol, J.-C., Carnaud, M., Boutterin, M.-C., and Girault, J.-A. (2003). PIAS1-mediated sumoylation of focal adhesion kinase activates its autophosphorylation. J. Biol. Chem. *278*, 47434–47440.

Kurenova, E., Xu, L.H., Yang, X., Baldwin, A.S., Jr., Craven, R.J., Hanks, S.K., Liu, Z.G., and Cance, W.G. (2004). Focal adhesion kinase suppresses apoptosis by binding to the death domain of receptor-interacting protein. Mol. Cell. Biol. *24*, 4361–4371.

Lewis, J.M., Truong, T.N., and Schwartz, M.A. (2002). Integrins regulate the apoptotic response to DNA damage through modulation of p53. Proc. Natl. Acad. Sci. USA *99*, 3627–3632.

Lietha, D., Cai, X., Ceccarelli, D.F., Li, Y., Schaller, M.D., and Eck, M.J. (2007). Structural basis for the autoinhibition of focal adhesion kinase. Cell *129*, 1177–1187.

McLean, G.W., Carragher, N.O., Avizienyte, E., Evans, J., Brunton, V.G., and Frame, M.C. (2005). The role of focal-adhesion kinase in cancer—a new therapeutic opportunity. Nat. Rev. Cancer *5*, 505–515.

Mitra, S.K., and Schlaepfer, D.D. (2006). Integrin-regulated FAK-Src signaling in normal and cancer cells. Curr. Opin. Cell Biol. *18*, 516–523.

Mitra, S.K., Mikolon, D., Molina, J.E., Hsia, D.A., Hanson, D.A., Chi, A., Lim, S.T., Bernard-Trifilo, J.A., Ilic, D., Stupack, D.G., et al. (2006). Intrinsic FAK activity and Y925 phosphorylation facilitate an angiogenic switch in tumors. Oncogene *25*, 5969–5984.

Oren, M. (2003). Decision making by p53: life, death and cancer. Cell Death Differ. *10*, 431–442.

Parsons, J.T. (2003). Focal adhesion kinase: the first ten years. J. Cell Sci. *116*, 1409–1416.

Reddig, P.J., and Juliano, R.L. (2005). Clinging to life: cell to matrix adhesion and cell survival. Cancer Metastasis Rev. *24*, 425–439.

Schober, M., Raghavan, S., Nikolova, M., Polak, L., Pasolli, H.A., Beggs, H.E., Reichardt, L.F., and Fuchs, E. (2007). Focal adhesion kinase modulates tension signaling to control actin and focal adhesion dynamics. J. Cell Biol. *176*, 667–680.

Shen, T.-L., Park, A.Y.J., Alcaraz, A., Peng, X., Jang, I., Koni, P., Flavell, R.A., Gu, H., and Guan, J.-L. (2005). Conditional knockout of focal adhesion kinase in endothelial cells reveals its role in angiogenesis and vascular development in late embryogenesis. J. Cell Biol. *169*, 941–952.

Slack-Davis, J.K., Martin, K.H., Tilghman, R.W., Iwanicki, M., Ung, E.J., Autry, C., Luzzio, M.J., Cooper, B., Kath, J.C., Roberts, W.G., and Parsons, J.T. (2007). Cellular characterization of a novel focal adhesion kinase inhibitor. J. Biol. Chem. *282*, 14845–14852.

Stewart, A., Ham, C., and Zachary, I. (2002). The focal adhesion kinase amino-terminal domain localises to nuclei and intercellular junctions in HEK 293 and MDCK cells independently of tyrosine 397 and the carboxy-terminal domain. Biochem. Biophys. Res. Commun. *299*, 62–73.

Stromblad, S., Becker, J.C., Yebra, M., Brooks, P.C., and Cheresh, D.A. (1996). Suppression of p53 activity and p21WAF1/CIP1 expression by vascular cell integrin alphaVbeta3 during angiogenesis. J. Clin. Invest. *98*, 426–433.

Tsukada, T., Tomooka, Y., Takai, S., Ueda, Y., Nishikawa, S., Yagi, T., Tokunaga, T., Takeda, N., Suda, Y., Abe, S., et al. (1993). Enhanced proliferative potential in culture of cells from p53-deficient mice. Oncogene *8*, 3313–3322.

Vousden, K.H. (2002). Activation of the p53 tumor suppressor protein. Biochim. Biophys. Acta *1602*, 47–59.

Molecular Cell, Volume *29*

Supplemental Data

Nuclear FAK Promotes Cell Proliferation and Survival through FERM-Enhanced p53 Degradation

Ssang-Taek Lim, Xiao Lei Chen, Yangmi Lim, Dan A. Hanson, Thanh-Trang Vo, Kyle Howerton, Nicholas Larocque, Susan J. Fisher, David D. Schlaepfer, and Dusko Ilic

Supplemental Experimental Procedures

DNA constructs and mutagenesis

pEGFP-FAK and pEGFP-FRNK were as described (Ilic et al., 1998). FAK FERM (1-402) was cloned into pEGFP-C1 (BD Biosciences) by generating HindIII and BamHI sites by PCR (see supplemental Table1 for PCR primers). Quickchange (Stratagene) site-directed or PCR mutagenesis was used to K152R, R177A/R178A, K190A/K191A, K204A/K205A, K216A/K218A, R311A/K312A within pEGFP-C1 FAK FERM. Mutations were transferred into pEGFP-C1 FAK by replacement of EcoRI/ClaI fragments. FAK FERM F1 (33-132), FERM F2 (128-253), and FERM F3 (253-353) lobe sequences were amplified by PCR and cloned into the pEBG mammalian GST fusion expression vector. All constructs were verified by sequencing. pGEX-p53 and HA-Mdm2 were from P. Sun (Scripps). Flag-tagged p53 was generated by subcloning of BamHI/Klenow-filled EcoRI fragments from pGEX-p53 into BamHI/SmaI sites of p3XFLAG-CMV7.1 (Sigma). pCW7-Myc-ubiquitin was from R. Kopito (Stanford). WWP-Luc (2.4 kb wild-type p21WAF1 promoter-luciferase) and DM-Luc (deletion mutation in p53 binding site in p21WAF1 promoter) were from G. Wahl (The Salk Institute).

RNA interference and lentivirus

Human FAK and scrambled shRNA were used as described (Mitra et al., 2006a). Mouse Pyk2 shRNA (see supplemental Table 1 for sequence) was cloned into pLentiLox3.7 and human p53 siRNA were from Dharmacon, and 100 pmol siRNA were transfected in 6 well with Lipofectamine 2000 (Invitrogen). FAK FERM or FRNK constructs were cloned into the NheI/SwaI or NheI/BamHI sites of pCDH-MCS1 lentiviral vector, respectively (System Biosciences). Lentiviral production and target cell infection were as described (Mitra et al., 2006a).

Adenovirus and retrovirus

HA-tagged FAK WT, FAK F397, FAK KD (R454), FAK Pro- (Ala-712, 713, 872, 873, 876, and 877), FAK Δ1-100, FRNK, and Myc-FAK-FERM (1-402) was created using a Tet-transactivator (TA) system as described (Mitra et al., 2006a). Cells were infected with 5 plaque forming units (pfu)/cell for Ad-TA (Mock control) and with 5 Ad-TA plus 50 pfu/cell Ad-FAK constructs. NheI-MluI fragments of pEGFP-C1 FAK FERM and FRNK were cloned into EcoRV site of pCMV-Shuttle (Stratagene). Ad Myc-FERM R177/R178 was generated by replacing GFP with Myc by PCR from pCMV-Shuttle GFP-FERM R177/R178. Adenovirus was produced using the AdEasy system (Stratagene). Cells were infected with 50 pfu/cell GFP or GFP-FAK FERM constructs and analyzed after 48 h. NheI/BamHI fragments of GFP, GFP-FAK WT, GFP-FAK R177A/R178A, GFP-FAK FERM 1-402, GFP-FAK FERM 1-402 F397 from pEGFP-C1 were

cloned into SnaBI site of pBabe-Puro. Retrovirus production and target cell infection were as described (Mitra et al., 2006b). Early passage FAK-/- MEFs were infected, selected with 1 µg/ml puromycin, and pooled populations of GFP-positive cells were isolated by sorting.

p53 activity

Early passage FAK-/-p21-/- MEFs were infected with 50 pfu/cell Ad-FAK, Ad-FERM, or Ad-FRNK. After 16h, cells were co-transfected (Lipofectamine 2000) with 0.1 µg WWP-Luc and 5 ng pTK-Renilla luciferase (Promega). For experiments in FAK-/-p53-/- MEFs in 6-well plates, 1.2 µg pEGFP-FAK, 0.25 µg Flag-p53, 0.1 µg WWP-Luc, and 5 ng pTK-Renilla were co-transfected (Lipofectamine 2000). For control points, pCDNA3.1 plasmid was added to equalize total DNA. Endogenous or transfected p53 activity was measured at 48 h using the dual-luciferase assay kit (Promega), a luminometer (TD-20/20 model, Turner Design), and final values corrected for transfection efficiency as determined by Renilla luciferase activity.

p53 turnover and ubiquitination

Confluent FAK+/+p21-/- and FAK-/-p21-/- MEFs were incubated in methionine- and cysteine-free MEM (Gibco) for 30 min, 1.0 mCi/ml L-[^{35}S]methonine, L-[^{35}S]cysteine (Amersham Pharmacia Biotech) was added for 1 h, cells washed 2X with normal media, and incubated for the indicated times prior to modified RIPA cell lysis. Cells were transduced with various amounts of Ad-FAK or Ad-FERM for 48 h prior to [^{35}S]methonine labeling or cell lysis. p53 was immunoprecipated (PAb240 and CM5) overnight at 4˚C, complexes collected with GammaBind Plus Sepharose (Amersham), analyzed by SDS-PAGE, gels were fixed, treated with Fluorohance (RPI), dried, and exposed to BioMax MS Imaging film (Kodak). p53 bands were quantified by densitometry. To evaluate ubiquitin incorporation into p53, co-transfection experiments were performed in Mdm2-/-p53-/- or Mdm2+/+p53-/- MEFs or in human HEK293 cells. For 293 cells, 1µg Flag-p53, 0.5 µg Myc-ubiquitin, and 5 µg FAK, FERM, or FRNK plasmid DNA were used. MG132 (40 µM) was added 3 h prior cell lysis for ubiquitin analyses. Flag-p53 was isolated by IP and visualized by anti-ubiquitin (FK-2) blotting.

Cell proliferation and apoptosis

Human diploid BJ fibroblasts and HUVECs were infected with scrambled or FAK shRNA lentivirus, plated onto gelatin-coated glass slides, and cell proliferation measured after 72 h by incubation with 10 µM BrdU for 16 h. Cells were fixed with 3.7% paraformaldehyde, permeabilized with 0.1% Triton X-100, and incubated with anti-BrdU (Roche) for 1 h at 37°C followed by Texas-red goat anti-mouse for 30 min. Cell apoptosis determined after lentivirus infection (4 days) by FACS using the Annexin V and 7-actinomycinD (7-AAD) staining kit (BD Pharmingen). Quadrant gates were positioned based upon the autofluorescence of unstained cells and single stained cells in FL2 and FL3 channels. Lentivirus-infected BJ fibroblast apoptosis in the presence or in the absence of 20 µg/ml cisplatin was also measured by TUNEL staining using the TMR red kit (Roche). For BrdU and TUNEL staining, red and green fluorescence images were captured at 10X and single GFP or double-positive GFP-Red cells were enumerated.

Supplemental References

Ilic, D., Almeida, E.A., Schlaepfer, D.D., Dazin, P., Aizawa, S., and Damsky, C.H. (1998). Extracellular matrix survival signals transduced by focal adhesion kinase suppress p53-mediated apoptosis. J. Cell Biol. *143*, 547-560.

Mitra, S.K., Lim, S.T., Chi, A., and Schlaepfer, D.D. (2006a). Intrinsic focal adhesion kinase activity controls orthotopic breast carcinoma metastasis via the regulation of urokinase plasminogen activator expression in a syngeneic tumor model. Oncogene *25*, 4429-4440.

Mitra, S.K., Mikolon, D., Molina, J.E., Hsia, D.A., Hanson, D.A., Chi, A., Lim, S.T., Bernard-Trifilo, J.A., Ilic, D., Stupack, D.G.*, et al.* (2006b). Intrinsic FAK activity and Y925 phosphorylation facilitate an angiogenic switch in tumors. Oncogene *25*, 5969-5984.

Table S1. Primers used for PCR cloning, PCR mutagenesis and Pyk2 shRNA.

Primer	Sequence	Note
FAK_HindIII-5'	5'-CCCaagcttCCATGGCAGCTGCTTATCTTGACCC-3'	FAK 1-402 cloning
FAK_BamHI-3'	5'-GGGggatccTCACTCATCGATGATCTCTGCATAG-3'	FAK 1-402 cloning
FAK_Y397F_BamHI-3'	5'-GGGggatccTCACTCATCGATGATCTCTGCA**A**AG-3'	FAKY397F 1-402 cloning
FAK_K152R_BspEI-5'	5'-CGCGGtc**cg**gaGTGACTACATGCAAG-3'	Paired with FAK_HindIII-5'
FAK_K152R_BspEI-3'	5'-CGGtc**cg**gaCCTGTTGATAGAAGAAATTCAATGTTGGC-3'	Paired with FAK_BamHI-3'
FAK_R177/R178A-5'	5'GTTGGGTTGTTTGGAAATT**GC**G**GC**ATCCTATTGGGAGATGA GGGG3	Quickchange mutagenesis
FAK_R177/R178A-3'	5'CCCCTCATCTCCCAATAGGAT**GC**C**GC**AATTTCCAAACAACC CAAC3'	Quickchange mutagenesis
FAK_K190/K191A_XhoI-5'	5'-GCCctcgag**GC**G**GC**GTCCAACTATGAAGTATTAGAAAAAGAT GTTGG-3'	Paired with FAK_HindIII-5'
FAK_K190/K191A_XhoI-3'	5'-CGCctcgagGGCATTACCCCTCATCTCCC-3'	Paired with FAK_BamHI-3'
FAK_R312/K313A-5'	5'-CAGTGAAGACAAAGAC**GC**G**GC**AGGTATGCTACAACTC-3'	Quickchange mutagenesis
FAK_R312/K313A-3'	5'-GAGTTGTAGCATACCT**GC**C**GC**GTCTTTGTCTTCACTG-3'	Quickchange mutagenesis
FAK_K204/R205A-5'	5'-TTAGAAAAAGATGTTGGTTTA**GC**G**GC**ATTTTTTCCTAAGA GTTTAC-3'	Quickchange mutagenesis
FAK_K204/R205A-3'	5'-GTAAACTCTTAGGAAAAAAT**GC**C**GC**TAAACCAACATCTTTTT CTAA-3'	Quickchange mutagenesis
FAK_F1_BamH1-5'	5'-GACCggatccATGGAACGAGTATTAAAGGTC-3'	FERM F1 33-132 cloning
FAK_F1_SmaI-3'	5'-TTTcccgggTCATCCTTTTGGCAAGTAACGAAT-3'	FERM F1 33-132 cloning
FAK_F2_BamH1-5'	5'-AAAggatccTACTTGCCAAAAGGATTTC-3'	FERM F2 128-253 cloning
FAK_F2_NotI-3'	5'-TTTgcggccgcTCAAAATCTGTACACAGGAGA-3'	FERM F2 128-253 cloning
FAK_F3_BamH1-5'	5'-AAAggatccTTTGACAAAGAGTGCTTCAAGTG-3'	FERM F3 253-353 cloning
FAK_F3_NotI-3'	5'-TTTgcggccgcTTATCCATTCACCAGCCGGCAGTAT-3'	FERM F3 253-353 cloning
Pyk2 shRNA-5'	5'-*t*GAAGTAGTTCTTAACCGCA*ttcaagaga*TGCGGTTAAGAACTA CTTC*ttttttc*-3'	Pyk2 shRNA cloning
Pyk2 shRNA-3'	5'-TCGA*gaaaaaa*GAAGTAGTTCTTAACCGCATC*tctcttgaa*TGCGG TTAAGAACTACTTC*a*-3'	Pyk2 shRNA cloning 5'TCGA is XhoI overhang

Lower characters represent restriction enzyme site. Mutated nucleotides are bold. 5' primer represents forward and 3' for reverse primers. Italicized characters are accessory components of shRNA. Underlined represents stop codons. FAK K152R, K190/K191A, and R312/K313A are generated by three-fragment ligation with PCR products and pEGFPC1 vector.

Table S2. Ratio of nuclear to cytoplasmic GFP-FAK or GFP FAK-FERM.

Data from Fig. 4D

	DMSO	Leptomycin B
FAK wild-type	0.4 +/- 0.1	2.3 +/- 0.4
FAK R177A/R178A	0.6 +/- 0.1	0.5 +/- 0.1

Data from Fig. 5D and E

	DMSO	Staurosporine
FAK wild-type	0.6 +/- 0.1	4.4 +/- 0.9
FAK R177A/R178A	1.2 +/- 0.5	1.4 +/- 0.5

Data from Fig. 6A

FAK FERM wild-type	1.9 +/- 0.2
FAK FERM K152R	1.7 +/- 0.2
FAK FERM R177A/R178A	0.7 +/- 0.1
FAK FERM K190A/K191A	1.3 +/- 0.1
FAK FERM R312A/K313A	2.0 +/- 0.4
FRNK	1.3 +/- 0.2

Image J (v1.36b) was used to obtain GFP fluorescence pixel intensity values from equal areas of nuclear and cytoplasmic region of cells and is shown as a nuclear/cytoplasmic ratio from at least 10 randomly-selected cells. Values are means +/- SD.

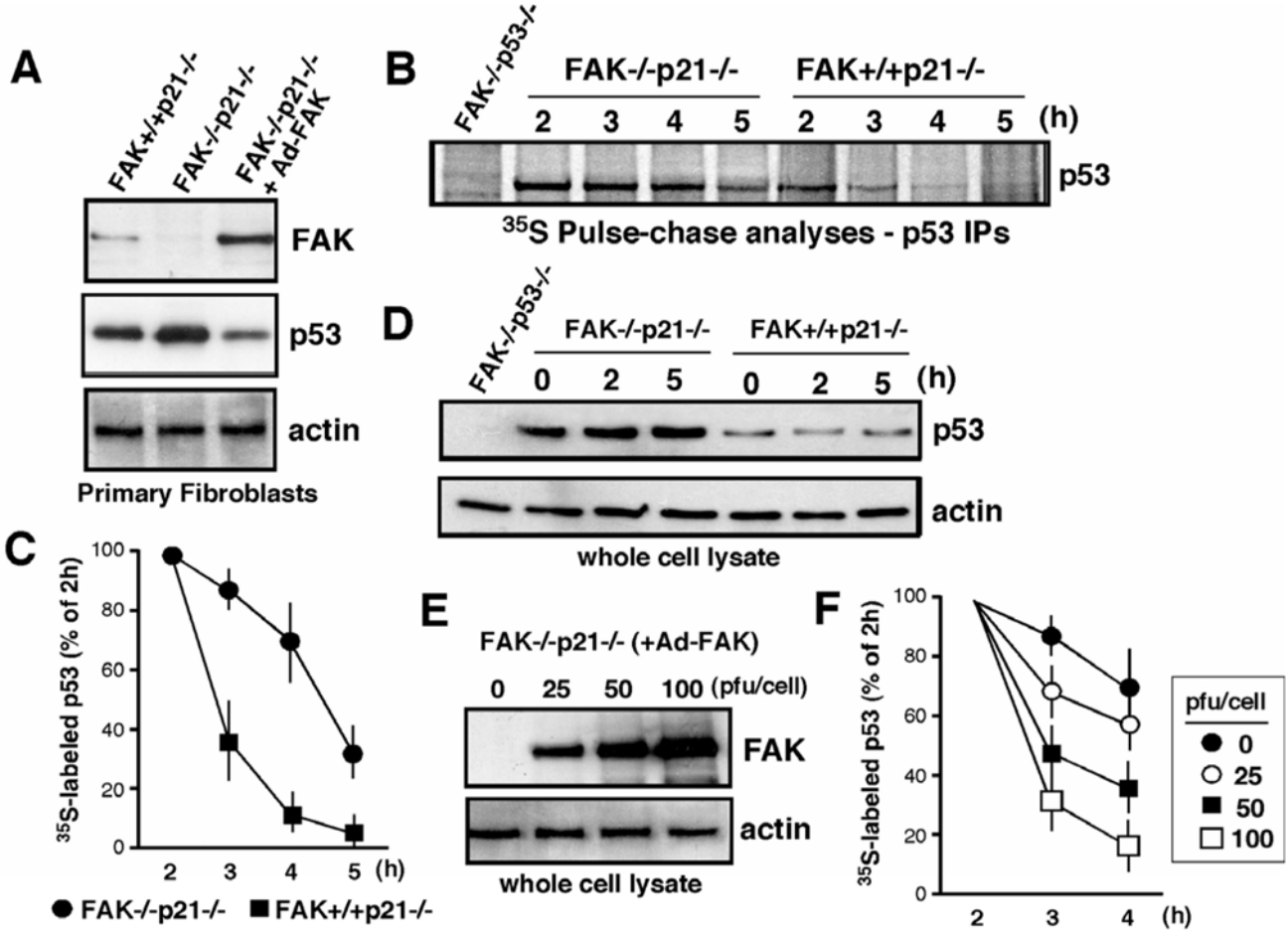

Supplemental Figure 1. FAK promotes p53 turnover. **(A**) p53 expression is elevated in FAK-/-p21-/- fibroblasts compared to FAK+/+p21-/- cells. Transient Ad-FAK expression in FAK-/-p21-/- cells decreases steady-state p53 levels as determined by immunoblotting. **(B)** Pulse-chase [35S]-labeling of FAK+/+p21-/- and FAK-/-p21-/- cells shows increased p53 turnover in cells with FAK. Shown is an autoradiograph of 35S-labeled p53 immunoprecipitated from 2 to 5h after pulse-labeling. **(C)** Quantitation of p53 decay rate in cells with FAK. As shown in panel B, the p53 band intensity at the 2h time point from either FAK-/-p21-/- or FAK+/+p21-/- cells were used as 100%. Mean values +/- SD from three independent experiments. **(D)** Total steady-state p53 levels in FAK-/-p21-/- and FAK+/+p21-/- cells did not change during pulse-chase labeling as determined by immunoblotting. **(E**) Cells were transduced with the indicated pfu/cell Ad-FAK resulting in increased FAK expression by immunoblotting. **(F)** Transient FAK expression in FAK-/-p21-/- cells promotes increased p53 turnover in a dose-dependent manner. After 48h, cells were pulse-labeled, and p53 isolated by immunoprecipitation at hourly time points as described above. The p53 band intensity from the 2h point of each Ad-FAK condition was used as 100%. Mean values +/- SD from 3 independent experiments.

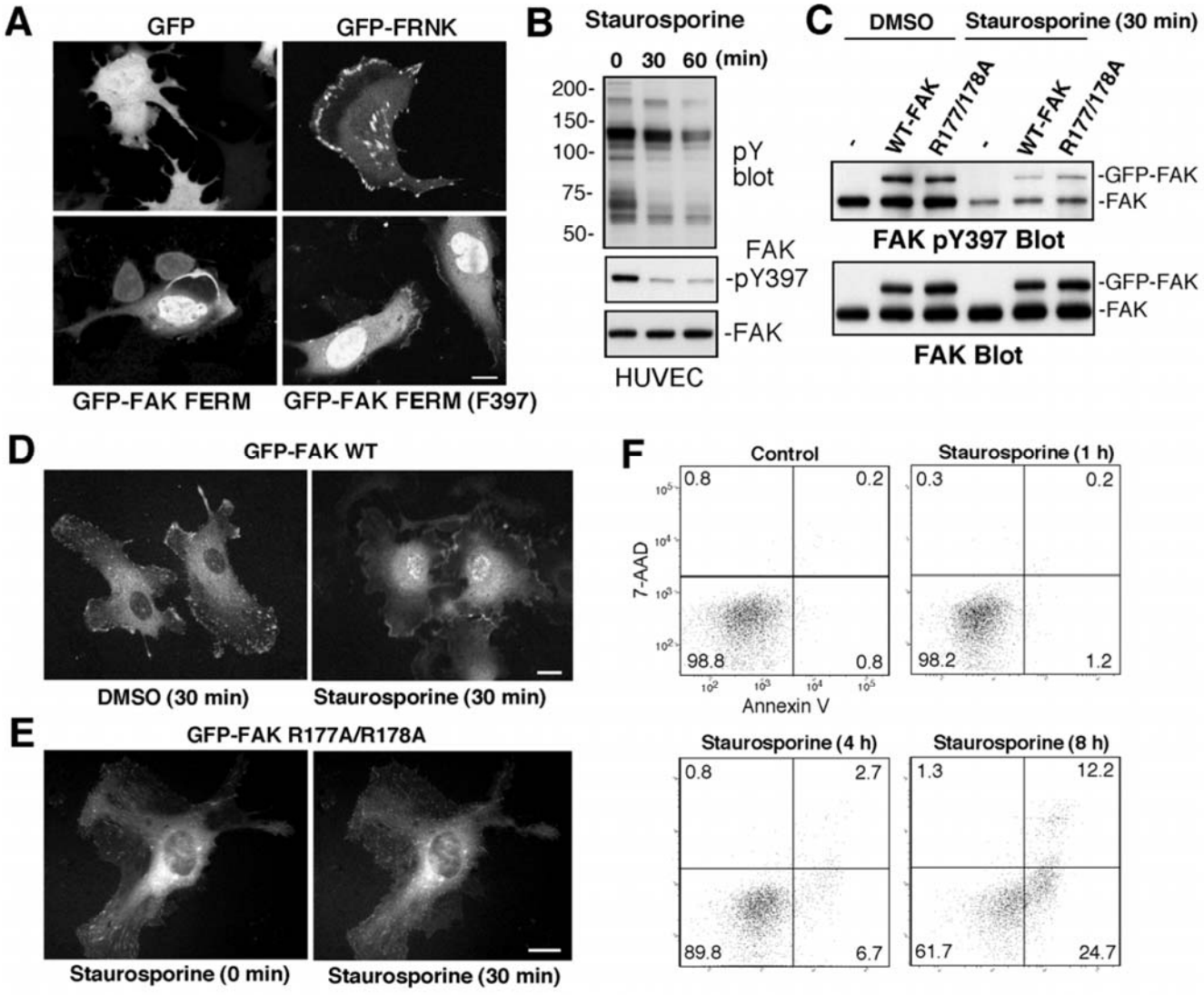

Supplemental Figure 2. Determinants and conditions promoting FAK nuclear accumulation. **(A)** Visualization of GFP-FAK FERM (1-402) in the nucleus and in membrane ruffles. FAK-/-p53-/- fibroblasts were transduced with the indicated retroviral constructs and GFP fluorescence visualized by confocal microscopy. **(B)** Anti-phosphotyrosine (pY) or phospho-specific FAK at Y397 (pY397) blotting of HUVEC lysates after staurosporine (1 μM) addition for the indicated times. Anti-FAK blotting shows that FAK is not degraded upon staurosporine addition. **(C)** Staurosporine promotes WT and R177/178A FAK dephosphorylation. GFP-FAK WT or GFP-FAK R177/178A were expressed via lentivirus infection of HUVECs. Cells were treated with DMSO or 1 μM staurosporine for 30 min, GFP- and endogenous FAK immunoprecipitated, and blotted with either phospho-specific FAK (pY397) or total FAK antibodies. **(D)** Staurosporine promotes GFP-FAK nuclear localization. HUVECs were treated with staurosporine (1 μM, 30 min) or DMSO, briefly fixed in paraformaldehdye, and GFP-FAK visualized by confocal microscopy. Scale bar is 10 μm. **(E)** Live cell imaging was used to follow GFP-FAK R177/178A distribution upon 1 μM staurosporine addition. Scale bar is 10 μm. **(F)** Staurosporine-induced HUVEC apoptosis was monitored by FACS with Annexin and 7-AAD staining.

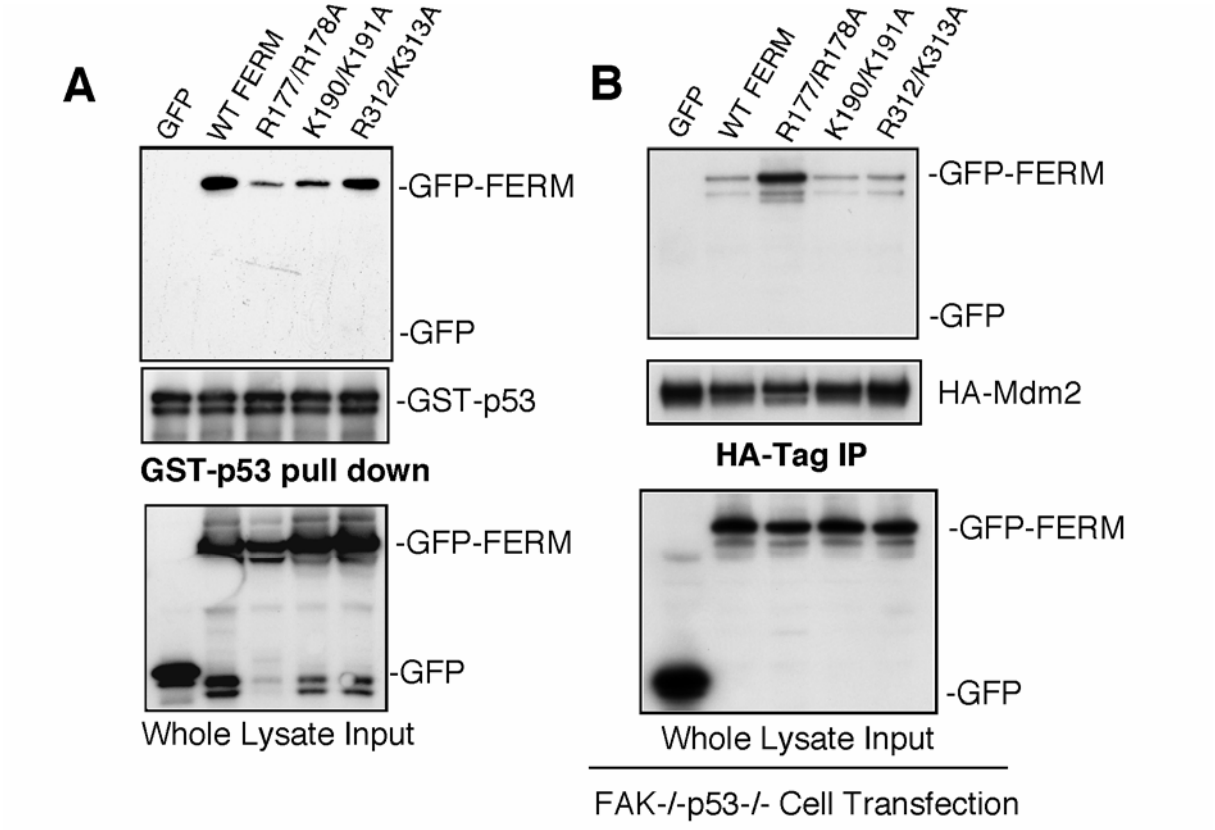

Supplemental Figure 3. FAK FERM binding to p53 and Mdm2. **(A**) FAK FERM mutation weakens p53 binding. 293T cells were transfected with GFP-FERM constructs, and lysates were subjected to GST-p53 pull-down assay. Lysates or GST-p53 pull-down were resolved by SDS-PAGE and blotted with anti-GFP and GST. **(B)** FAK FERM binds Mdm2 in the absence of p53. GFP-FERM constructs and HA-Mdm2 were co-transfected into FAK-/-p53-/- MEFs. MG132 was treated 3h prior lysis, HA-tag IP (clone 3F10) was performed. Lysates and IP were resolved by SDS-PAGE and blotted with anti-GFP and HA-tag.

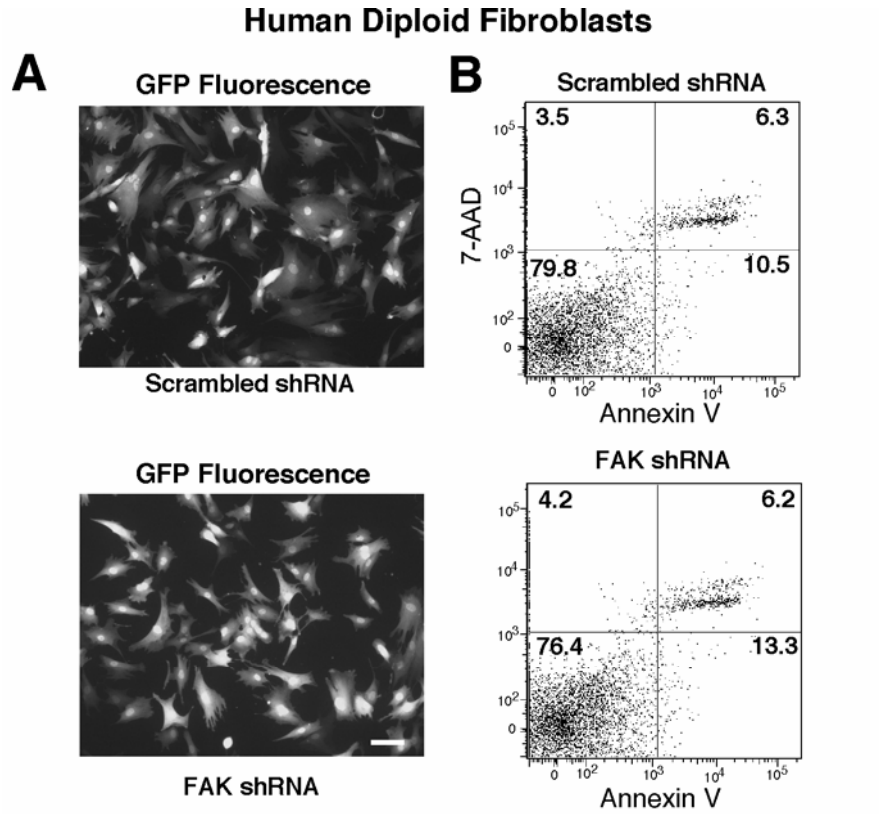

Supplemental Figure 4. Lentiviral shRNA transduction of human fibroblasts. **(A)** Anti-FAK or scrambled shRNA expression in human diploid fibroblasts does not change cell morphology. Lentiviral-associated GFP expression as a marker for shRNA-expressing cells after 72 h. Scale bar is 200 μm. **(B)** FAK shRNA does not increase human fibroblasts apoptosis as confirmed by FACS analysis with Annexin V and 7-AAD staining.

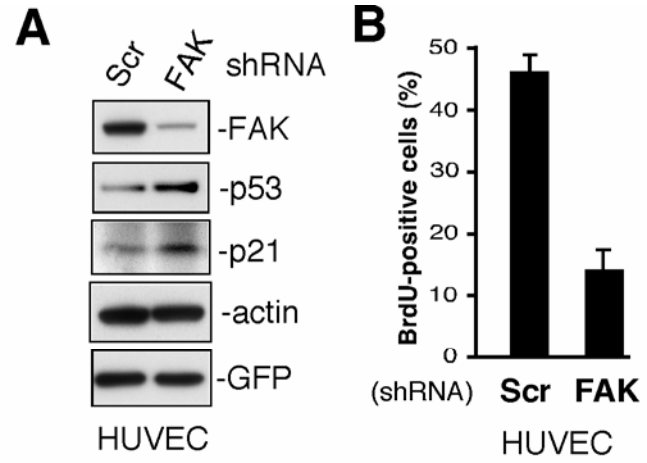

Supplemental Figure 5. FAK knockdown increases p53 and p21 levels and slows HUVEC cell proliferation. **(A)** Lysates from scrambled (Scr) and FAK shRNA infected HUVECs after 72 h were analyzed by anti-FAK, p53, p21, actin, and GFP blotting. **(B)** Cells were infected with the indicated lentivirus for 72 h, BrdU was added for 16h in growth media, cells were fixed, and stained with anti-BrdU antibody. Mean values +/-SD are percent of total GFP-positive cells.